

OVERDUE FINES: 25¢ per day per item

RETURNING LIBRARY MATERIALS: Place in book return to remor charge from circulation recor

1 mg ( 2 1995)

# THE ENERGETICS AND BIOMECHANICS OF SWIMMING IN THE MUSERAT (ONDATRA ZIBETHICUS) WITH HYDRODYNAMIC CONSIDERATIONS

Ву

Frank E. Fish

A DISSERTATION

Submitted to

Michigan State University

in partial fulfillment of the requirements

for the degree of

DOCTOR OF PHILOSOPHY

#### **ABSTRACT**

THE ENERGETICS AND BIOMECHANICS OF SWIMMING IN THE NUSKRAT (ONDATRA
ZIBETHICUS), WITH HYDRODYNAMIC CONSIDERATIONS

Ву

### Frank E. Fish

The surface swimming of muskrats (<u>Ondatra zibethicus</u>) was studied by forcing individual animals to swim against a constant water current, of velocity ranging from 0.2 to 0.75 m/s, in a recirculating water channel. The swimming muskrat was enclosed in a metabolic chamber to monitor oxygen consumption as a measure of the aerobic power input, while lateral and ventral views of the animal were filmed simultaneously for analysis of thrust by the propulsive appendages.

The metabolic rate ( $V_{02}$ ) of swimming muskrats at a water temperature of 25°C was found to increase linearly over the range of test velocities from 0.2 to 0.75 m/s. At higher velocities increased power input was probably be supplied through anaerobic metabolism. A similar trend in  $\dot{V}_{02}$  was observed for muskrats swimming in water at 30°C, but at a significantly lower level. The higher  $\dot{V}_{02}$  at 25°C was due to the maintenance of thermoregulation below thermoneutrality in response to the interaction of ambient temperature, convection, thermal conductivity of water, and

activity state of the animal.

Drag measurements and flow visualization on dead muskrats demonstrated that these animals experience large resistive forces due to the formation of waves and a turbulent wake, because of the pressure and gravitational components which dominate the drag force.

Biomechanical analysis demonstrated that thrust is mainly generated by alternate strokes of the hindfeet in the paddling mode. A general lengthening of the hindfoot and presence of lateral fringe hairs on each digit increase the surface area of the foot to product thrust more effectively during the power phase of the stroke cycle. Drag on the foot during the recovery phase is minimized by configural and temporal changes of the hindfoot. Increased thrust with increasing velocity of the muskrat is produced by an increase in the arc through which the hindfeet are swept. However, the frequency of the stroke cycle remains relatively constant across all velocities at a level of 2.5 Hz. Such a constant stroke frequency suggests the possibility of a resonant system.

Travelling waves were observed to move posteriorly down the laterally compressed tail of the muskrat in synchrony with the hindfoot stroke cycle. Although the lateral undulations of the tail were analogous to anguilliform locomotion in fish, the thrust generated by the tail represented only 1.4 percent of the thrust power generated by the hindfeet. It was shown that the tail is also important in reduction of drag by preventing yawing and potentially in modifying the water flow around the body.

The efficiency in terms of the metabolic and mechanical energy expended were lower than more aquatically adapted organisms. The minimum cost of transport for the muskrat was 13.5 times higher than for a similarly sized fish, but was comparable with the high costs for other endothermic surface swimmers which utilize paddling. The muskrat minimizes its energy expenditure while swimming by cruising at 0.6 m/s where the cost of transport is the low, the mechanical and aerobic efficiencies the high, and anaerobic component small.

In comparison to highly adapted aquatic organisms, the muskrat may be regarded as an inefficient swimmer due to its paddling mode of surface swimming. However, this animal is highly mobile both on land and in the water, so that its physiology and morphology should be viewed as a compromise between vastly different environments.

#### ACKNOWLEDGEMENTS

I wish to express my sincere appreciation to the members of my committee, Dr. James L. Edwards (chairman), Dr. Paul W. Webb, Dr. Richard W. Hill, and Dr. Rollin H. Baker for their advice, constructive criticism, and encouragement during the course of this study. I also wish to thank especially Dr. Robert W. Blake for this assistance in hydrodynamics and Edward Rybak for help in programming. I wish to thank Dr. C. D. McNabb, Dr. R. A. Pax, Dr. G. W. Bird and Joseph L. Erwin for use of facilities, and Martha Flanders and Miriam Zelditch for assistance with figures.

I am grateful to the Department of Zoology for financial support and to the American Society of Mammalogists and Sigma Xi for funding through student grants-in-aid. The State of Michigan, Department of Natural Resources are gratefuly acknowledged for allowing the collection of muskrats.

## TABLE OF CONTENTS

	page
LIST OF TABLES	iv
LIST OF FIGURES	v
INTRODUCTION	1
GENERAL BACKGROUND	4
The Animal	4
Swimming Biomechanics	5
Swimming Energetics	7
MATERIALS AND METHODS	8
Experimental Animals	8
Water Channel and Metabolic Chamber	8
Oxygen Consumption	12
Biomechanical Analysis	14
Drag Measurements	15
Flow Visualization	19
Statistical Procedure	19
RESULTS	21
Metabolic Response	21
Temperature Effects	21
Body Drag	25
Biomechanics	30
Flow Visualization	48

DISCUSSION	
Swimming Energetics	52
Temperature Effects	55
Drag and Power Gutput	58
Thrust, Power, and Energy	64
Efficiency and Cost of Transport	81
Aquatic Locomotory Adaptations	99
CONCLUSIONS	112
REFERENCES	115
APPENDIX	
A list of Symbols	127

# LIST OF TABLES

Tab	le	page
1.	Regressions for metabolic rates of muskrats	
	swimming at various velocities, U, and at	
	different water temperatures, $T_a$	24
2.	Mean tail wave parameters	78

## LIST OF FIGURES

Figure		page
1.	Experimental water channel. Arrows indicate the	
	direction of water flow which was driven by the motor	
	in the return channel. Broken lines illustrate the	
	lamimar flow grids () and Plexiglas walls () in	
	the working section of the water channel. MC represents	
	the metabolic chamber, EM, the electric motor, RC, the	
	return channel, WS, the working section, and EG, the	
	electric grid	10
2.	Drag balance. The three axes are indicated by $X$ , $Y$ , and	
	Z. $W_{\mbox{\scriptsize b}}$ represents the counterbalancing weight, B, the	
	mounting bracket used to hold the muskrat, and P, the	
	protractors. Procedure for use of the drag balance is	
	given in text	17
3.	Net mass-specific oxygen consumption of swimming	
	muskrats as a function of swimming velocity, U	23
4.	Mass-specific oxygen consumption, Net $\dot{v}_{0_2}$ , as a	
	function of swimming velocity, U, for muskrats in	
	water temperatures of 25 ( $\bullet$ $\longrightarrow$ ) and 30 ( $\circ$ $\bullet$ $\bullet$ $\bullet$ $\bullet$ ) °C	27

Fis	ure	page
5•	Drag as a function of water velocity, U. The regression	
	line is given in the text by equation (2). Symbols	
	indicate drag for individual muskrats	29
6.	Diagrammatic representation of the lateral view of the	
	hindfoot through the stroke cycle. The alternate	
	sequential frames are indicated by the numbers for each	
	foot position, where the power phase is indicated by	
	frames 15-21 and the recovery phase by frames 5-13. The	
	segments of the foot shown are the phalanges,	
	metatarsals, tarsals, and tibia. The angle shown on	
	each limb tracing represents the ankle joint	33
7.	The angular velocity ( $w$ ) of the power and recovery	
	phases of the hindfoot as plotted over the time of one	
	stroke cycle for a muskrat swimming at 0.45 m/s	35
8.	The stroke frequency of the hindfeet as a function of	
	the swimming velocity, U	38
9.	The arc of the hindfoot plotted as a function of the	
	swimming velocity, U	40
10.	The angle of the hindfoot to the long axis of the body	
	at the beginning (O) and $end(\bullet)$ of the power phase	43
11.	The force on isolated hindfeet determined by drag	
	measurements in the power phase $(F_p)$ , power phase	
	with fringe hairs removed (Fp'), and recovery phase	
	$(F_R)$ as plotted against the water flow velocity, u	45

Figu	re	page
12.	Sequential tracings of the tail of a complete propulsive	
	cycle for a muskrat swimming at 0.5 m/s. Frames of film	
	are indicated for each tail position	47
13.	Plot of the amplitude at the tip of the tail as a	
	function of the swimming velocity, U	50
14.	The drag power output of the muskrat, $P_0$ , as a	
	function of the swimming velocity, U	63
15.	Schematic diagram of the hindfeet during the power and	
	recovery phases showing the orientation angles, $\gamma$ and $\gamma'$	,
	and the centers of action, $C_A$ and $C_A$ . The	
	acetabular, knee, and ankle joints are represented by A,	
	B, and C, respectively	68
16.	The mean power expended during the power $(-)$ , $\overline{W}_p$ , and	
	recovery (), $\overline{W}_{r}$ , phases for one paddle as a function	
	of the swimming velocity, U	71
17.	The thrust power generated by the tail, $P_{T}$ , as a	
	function of the swimming velocity U	80
18.	Comparison of the logs of energies ( $E_{M}$ , $E_{tot}$ ,	
	$E_{\text{th}}$ , $E_{\text{D}}$ ) expended at various swimming velocities,	
	C	83
19.	The logs of efficiencies $(\eta_{me}, \eta_{e}, \eta_{aerob})$	
	as a function of swimming velocity, U	86

Figure		page
20.	The gross cost of transport as plotted against	
	swimming velocity, U. The dotted line represents the	
	cost of transport calculated from the regression of	
	total $v_{0_2}$ from Table 1A. The solid dots represent	
	the mean values over the range of $0.2$ to $0.75$ m/s.	
	The vertical lines represent + one standard error	
	(SE)	91
21.	Numbers of observations of muskrats swiming in a	
	large pond over a range of velocities. The single	
	observation represented by the stippled area was for	
	an animal observed swimming while carrying food	94
22.	Comparison of the minimum cost of transport over a range	
	of body masses. Discussion and symbols are given in the	
	text······	98
23.	Illustration of the flow around a circular body	
	with (A) and without (B) a splitter plate	106

#### INTRODUCTION

An aquatic animal propelling itself a unit distance at a constant velocity must supply a force which is equal to the sum or the resistance forces, or drag for swimming locomotion. The energy necessary to overcome the resistive forces is supplied from the metabolism of the animal. The metabolic expenditure represents the power input produced by the animal available to do work on its surroundings, while the power output is the realized energetic portion that performs work opposing the resistive forces. The metabolic power input can be empirically obtained by measuring the steady-state oxygen consumption of the animal while it is moving at a known constant velocity providing the exercise is aerobically supplied. The ratio of the mechanical power output to the metabolic power input determines the efficiency of energy utilization.

Another approach to the question of locomotor efficiency, including swimming, is the concept of the cost of transport. The cost of transport represents the metabolic energy per gram body mass necessary to move a unit distance, and can be used as a measure of the effectiveness of an active metabolism (Tucker, 1970). Animals with low costs of transport are metabolically more efficient at traversing a given distance than animals with high costs of transport. For a given body size, bony fish are reported

to have the lowest minimum cost of transport of any animal (Tucker, 1975). The energetic costs of locomotion have been determined mainly for terrestrial invertebrates and vertebrates (Schmidt-Nielsen, 1972a; Tucker, 1975), but for swimming animals energy costs have been measured almost entirely for fish (see review by Webb, 1975a).

In the case of mammals, the energetics of swimming have been empirically investigated only in sea lions (Costello and Whittow, 1975; Kruse, 1975) and humans (Holmer, 1972; DiPrampero et al., 1974).

Several attempts have been made to use estimates of drag to determine the maximum power output of cetaceans during swimming (Gray, 1936; Kermack, 1948; Parry, 1949; Lang, 1975). However, these estimates have been based on a number of questionable assumptions such as 100 percent efficiency in the muscles, inadequate data such as uncertain swimming speed, unknown flow conditions, and computations of resistance forces based on an idealized, submerged static body shape. This last assumption is of greatest concern in that it does not take account of the animal's propulsive undulations of the body, its mechanics, or surface effects.

Similar problems apply to all swimming mammals and the direct measurement of oxygen consumption is a preferred method for the determination of the aerobically supplied energy available for propulsion. Also, mechanical analysis of thrust, rather than drag, should be used to calculate the energy necessary for propulsion, in that propulsive movements of the appendages are taken into account.

A rigorous analysis of the development of metabolic and mechanical power for aquatic mammals has not previously been undertaken. The large size of many of these animals (e.g., cetaceans, sirenians, pinnipeds) precludes the possibility of easily obtaining such data. Alternatively, due to its small size, the muskrat can serve as a manageable model for the examination of the development and utilization of power for swimming locomotion. Combining a biomechanical analysis of the paddling mode of the muskrat (Mizelle, 1935) with physiological data allows an integrated approach to the study of aquatic adaptations. The functions of specific aquatic adaptations such as stiff hairs on the hindfeet, non-wettable fur, and a laterally compressed tail can also be studied.

Additionally, the muskrat affords the opportunity to examine the consequences of surface swimming. Little attention has been paid to this aspect of aquatic locomotion despite the number of non-piscine vertebrate swimmers which are restricted to the surface by their need of gaseous oxygen for respiration. The forces encountered at the air-water interface are complex and larger than those for submerged swimmers. Thus surface swimming may be expected to influence the energy budget of the muskrat. Surface swimmers such as the sea turtle (Prange, 1976), duck (Prange and Schmidt-Nielsen, 1970), and humans (DiPrampero et al., 1974) have higher mass specific costs of transport than fish and hence have lower efficiencies of energy utilization during swimming; the reason for the large energetic expenditure is believed to be due to the energy lost to surface waves formed by the animals (wave drag) (Schmidt-Nielsen, 1972a).

#### GENERAL BACKGROUND

## The Animal

The muskrat (<u>Ondatra zibethicus</u>) is a semi-aquatic microtine rodent which inhabits fresh and brackish water marshes, lakes, ponds, rivers, and streams (Walker, 1975). In North America, the species ranges from Alaska and Labrador, southward to Louisiana and Texas, and westward to Arizona and Baja California (Hall and Kelson, 1959). Muskrats do not occur along the California, Georgia, or South Carolina coast, or in Florida. These animals have been extensively introduced into Europe.

The aquatic adaptations of the muskrat include a pelage of non-wettable fur, consisting of long course guard hairs and dense silky underfur. The fur affords the animal a large degree of thermal insulation (Johansen, 1962b; McEwan et al., 1974) and buoyancy (Johansen, 1962b). The long tail is sparsely haired and laterally compressed. The tail has been shown to perform an important function in thermoregulation (Johansen, 1962a; Fish, 1979). Modifications of the hindfeet for swimming include a fringe of long, stiff hair on both sides of each phalanx and foot, and a lateral twist of the ankle joint (Errington, 1962). The small eyes and ears are almost hidden in the fur.

## Swimming Biomechanics

Shore-dwelling muskrats which are in permanent residence seldom swim beyond 400 m into a lake or marsh to feed (Errington, 1962). In rough water, muskrats tend to swim submerged.

Muskrats swim on the surface by alternate strokes of the hindfeet (Howell, 1930; Kirkwood, 1931; Svihla and Svihla, 1931; Mizelle, 1935; Dagg and Windsor, 1972) with the forefeet held under the chin with the palms inward (Mizelle, 1935). However, Arthur (1931) reported that during leisurely swimming muskrats use the forefeet and hindfeet both alternately and simultaneously, while Johnson (1925) stated that the swimming muskrat uses its hindfeet simultaneously. Peterson (1950) observed a single muskrat to swim backward "using all four feet in a stroke that resembled the 'dog paddle' in reverse."

Observations on muskrat swimming which are the most detailed to date were reported by Mizelle (1935, pp. 23-24), who stated that: "The strokes of the hind feet were in almost a vertical plane, deviating approximately five to fifteen degrees to the outside of the plane. On the forward stroke the foot is folded up like that of a duck, thereby cutting down the braking power of the appendages on the return forward. On the backward stroke the digits are extended laterally so as to utilize the interdigital webbing to a maximum degree. The propelling movement of the hind limb comes principally from the ankle joint, but to a slight degree from the knee., Movement of the femur is imperceptible." Such observations were made on animals estimated to be swimming from 0.4 to 1.3 m/s.

Dagg and Windsor (1972) reported the period of the hindfoot stroke to be 0.07 - 0.09 seconds. Mordvinov (1977) found the hindfoot stroke rate increased from 1.6 to 2.7 Hz with increasing swimming speeds from 3.5 to 8.4 m/s.

The most controversial aspect of swimming in muskrats has been the use of the tail. Dugmore (1914) and Johnson (1925) contend that the swimming muskrat uses its tail as a scull to produce thrust. Arthur (1931) states that the tail is only used as a scull when the muskrat is swimming against a current. Mizelle (1935) reported that sculling movements of the tail were only observed during submerged swimming. Other authors, however, saw no apparent use of the tail as either a scull or a rudder (howell, 1930; Kirkwood, 1931; Svihla and Svihla, 1931).

The hydrodynamics of swimming muskrats have only recently been examined. Mordvinov (1974) investigated the character of the boundary layer flow for submerged muskrats swimming against a current and found it was turbulent for muskrats swimming at 0.1 m/s. At a speed of 0.8 m/s, a large region of the boundary layer was observed to separate from the surface of the posterior part of the body, forming vortices. Using the ratio of the area of the hindfoot to the total wetted surface area of the muskrat, Mordvinov (1976) found that the muskrat was probably less effective in aquatic locomotion than other semi-aquatic rodents, such as the beaver and nutria.

Although the osteology and myology of the muskrat have been described (Muller, 1952/53; Eble, 1954/55; Flaim, 1956), there has been no rigorous attempt to examine the role of the bones and

muscles in swimming or a true biomechanical analysis. Flaim (1956) contends that the modified pelvis, large processes on the hinged limb bones, and large muscles of the hind limb are adaptations to an aquatic habitat.

## Swimming Energetics

No direct metabolic data are available on the actual energetics of muskrat swimming. However, previous measurements have been made of post-dive oxygen consumption in muskrats. Fairbanks and Kilgore (1978) stated that physical activity such as swimming probably accounted for the majority of excess oxygen consumption after a dive. However, these authors believed that the energetic cost of swimming was not great in muskrats. Johansen (1962b) speculated that the buoyancy of the muskrat, due to the air entrapped in the non-wettable fur, would reduce energy expenditure during surface swimming.

Other metabolic data for the muskrat in water have been taken only for resting animals. Hart (1962) found the lower critical temperature of muskrats in water to be 30°C. Fish (1979) reported the resting metabolic rate of restrained muskrats to be 1.07 cc 02/g/hr at an ambient temperature of 30°C. This metabolic rate was comparable to rates reported by Hart (1962), but lower than rates reported by Shcheglova (1964) for both summer and winter acclimatized muskrats. Muskrats in water below 30°C show a steep increase in their resting metabolic rate (Hart, 1962; Fish, 1979).

#### MATERIALS AND METHODS

## Experimental Animals

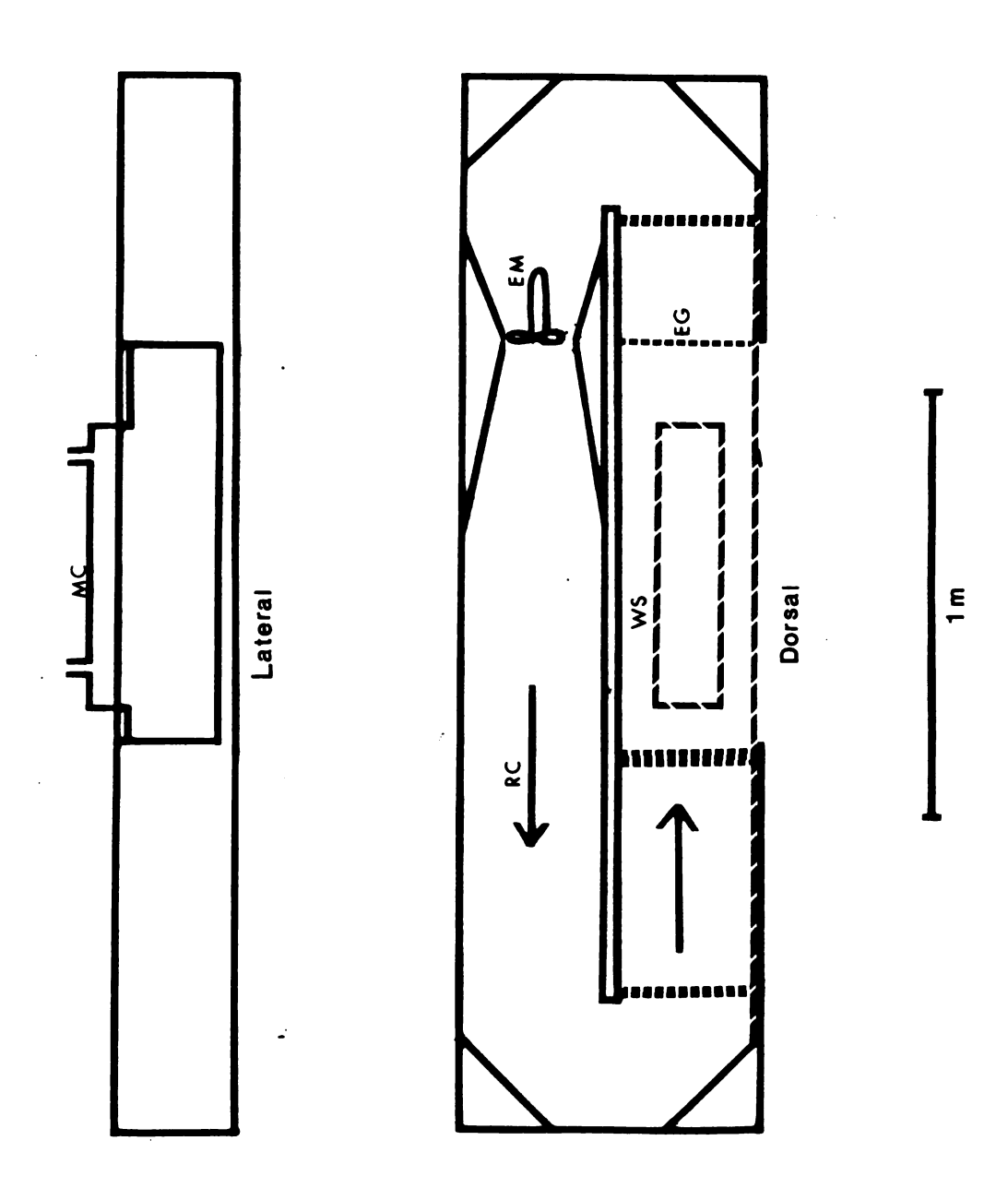
Ten muskrats (9 males and 1 female) were live-trapped in Ingham County, Michigan during the spring and summer of 1978 and 1979. The mean body mass of the muskrats was 648.9 g (range 530 - 1604 g) over the test period. To avoid mortality due to captivity throughout the period of testing, the animals were kept in large, outdoor concrete ponds at the Limnology Research Laboratory on the campus of Michigan State University. The ponds had a depth of approximately 2 m allowing unrestricted swimming and diving. Abundant aquatic vegetation, which grew in the ponds, was readily consumed by the muskrats and was used for bedding material. Apples supplemented the diet. The ponds were equipped with platforms above the water. Nest boxes were provided on the platforms and were modified for the capture of single animals when needed for testing.

## Water Channel and Metabolic Chamber

Experiments on swimming were conducted in a recirculating water channel (Fig. 1), based on Vogel and LaBarbera (1978). A working section (WS), in which a single muskrat was allowed to swim, was provided in the channel. The upstream end of the working

Figure 1. Experimental water channel. Arrows indicate the direction of water flow which was driven by the motor in the return channel. Broken lines illustrate the laminar flow grids (\*\*\*\*\*) and Plexiglas walls (\*\*\*\*\*\*) in the working section of the water channel.

MC represents the metabolic chamber, EM, the electric motor, RC, the return channel, WS, the working section, and EG, the electric grid.



section was bounded by a plastic grid (commercially termed "egg crate") in conjunction with a 5 cm wide grid of plastic straws, both of which removed turbulence from the water flow and also prevented the experimental animal from escaping. The downstream end of the working section was bounded with a low voltage electrified grid (EG) which prevented escape and stimulated steady swimming by the muskrat. Wires attached to the grid ran along the floor of the working section to prevent the experimental animal from standing on the floor to rest. The voltage was controlled with a Powerstat (Superior Electric Co.). All electricity was disconnected when the muskrat maintained steady swimming. During higher speed runs, a removable wall was placed in the working section to constrict its cross-sectional area and thus increase the water velocity when required. Plexiglas windows were installed in the side and bottom of the working section in order to allow observation and filming. In order to film simultaneous lateral and ventral views of the muskrat, a mirror was positioned under the ventral window at a 45° angle to reflect the ventral image of the muskrat toward the camera.

The top of the working section was formed by a Plexiglas metabolic chamber (MC) of the dimensions of 75.5 X 13.0 X 26.0 cm. Inlet and outlet air tubes entered through the walls of the chamber. The chamber was hinged to the inner wall of the water channel to allow for the introduction and removal of a muskrat. At its base, the metabolic chamber was equipped with a Plexiglas apron which extended over the working section. When the water channel was filled, the apron remained just below the water surface; thus

the base of the metabolic chamber was slightly submerged. This prevented any air leakage, but had little effect on the water flow. The dimensions of the metabolic chamber were large enough for a single muskrat to swim against a constant current without interference.

Water velocity, U (all symbols listed in Appendix A), was controlled by either a Sears 25 electric fishing motor (Model No. 217.590091) or a Mercury electric outboard motor (Model No. 10019) situated in the return channel (RC). Power to the motor was provided by a 12 V storage battery connected to a 6A battery charger. Motor speed was calibrated to water speed by determining the time a drop of ink or neutrally buoyant particle traversed a given distance.

Muskrats were tested at velocities ranging from 0.2 to 0.75 m/s. The arrangement of test velocities for each individual muskrat was such that there was no apparent order. Each muskrat was forced to swim steadily at a single test velocity for a period of 10 to 30 minutes to obtain sufficient data. During the initial exposure to the apparatus, each muskrat learned to swim steadily and avoid the downstream electrified grid within 15 min. Data were only collected during subsequent trials when the muskrat was proficient in swimming against current, so as to avoid biasing the results from excitation of the animals during the first trial runs.

## Oxygen Consumption

liass-specific oxygen consumption  $(\dot{v}_{0_2})$ , as a measure of

of metabolic rate, was monitored using an open-circuit system conforming to condition B of Hill (1972). The oxygen content of dry, CO<sub>2</sub>-free air flowing out of the metabolic chamber was monitored with a Beckman C-2 paramagnetic oxygen analyzer. Ascarite (A. H. Thomas Co.) and Drierite (W. A. Hammond Co.) were contained in tubes downstream of the metabolic chamber to absorb CO<sub>2</sub> and water vapor, respectively, from the air flow. The rate of air flow into the metabolic chamber was measured with a calibrated Gilmont Model 1300 flowmeter. The flow rate into the chamber was approximately 3.0 - 3.8 1/min for dry air at STP.

In order to obtain a realistic estimate of the energy expenditure of natural muskrat swimming, experimental animals were not fasted prior to testing in order to control for specific dynamic action, and animals swam in water at 25°C. After the experimental animal was placed in the metabolic chamber, the muskrat was given 10 to 30 minutes to adjust to the apparatus and water temperature. During this period, the resting metabolic rate was recorded for the animal. During the measurement of the resting  $\dot{v}_{0}$ , the animals floated quietly with approximately 33 percent of their surface area above the water. Although some paddling movements were observed, these tended to be infrequent and appeared not to influence  $\dot{v}_{0}$ .

To determine if diffusion of oxygen between the air flow and water contributed to a possible error in the measured oxygen consumption, a gas of known composition (88%  $N_2$ , 12%  $O_2$ ) was passed through the metabolic chamber with the water current at a single velocity. Any change in the gas composition was monitored

with the oxygen analyzer over a 30 minute period. Although Prange and Schmidt-Nielsen (1970) and Fish (1979) reported no significant error in studies involving an air-water interface, in the present study an error of approximately one percent was found at 0.7 and 0.75 m/s. This was due to the large turbulence produced by the motor. Apparent metabolic rates at 0.7 and 0.75 m/s were adjusted to compensate for this factor.

Tests to determine the effect of ambient temperature on the active  $\dot{V}_{02}$  were performed on four muskrats at water temperatures of 25 and 30°C. In contrast to the water temperature of 25°C, which was used for the bulk of the metabolic study, the 30°C water temperature was chosen because it represents the lower critical temperature for the muskrat in water (Hart, 1962).

# Biomechanical Analysis

Individual muskrats swimming over the range of test velocities were filmed at 24 and 50 frames/s with a Bolex H-16 SB motion picture camera equipped with a Kern Vario-Switar 100 POE zoom lens (1:1.9, f=16-100 mm) using 16 mm motion picture film (Kodak 4-X Reversal film 7277, ASA 320). The camera was driven with an ESM 12V DC motor. Lighting was supplied by three 250 W flood lamps surrounding the metabolic chamber. For analysis, sequential tracings of the propulsive appendages were made from the films using a stop-action projector (Lafayette Instrument Co. Model 00100) and light table.

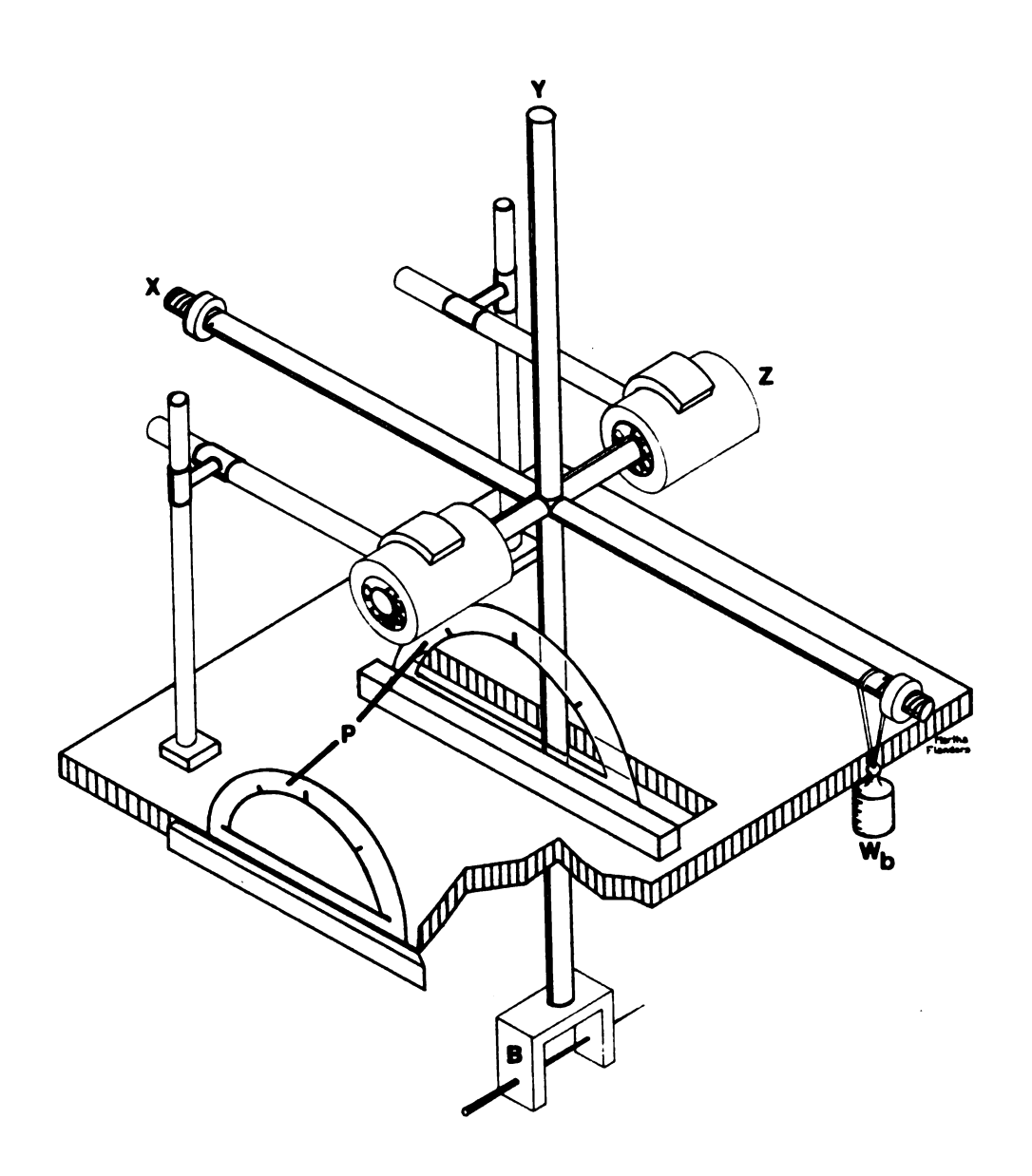
## Drag Measurements

Estimates of the total drag on the muskrat were made using dead-drag measurements. Since there is no appreciable flexion of the body of the muskrat during swimming (Mizelle, 1935), any error in the drag measurement would be mainly due to the movement of the appendages. Only the total drag was measured due to the complexity of separating the various drag components (frictional drag, pressure drag, wave drag) on a surface-swimming organism (Schmidt-Nielsen, 1972a).

Total drag measurements were made on seven dead muskrats, which were frozen into a natural swimming postures with the forelegs tucked under the chin and the tail stretched out straight. The hindlegs were removed for separate drag measurements. When placed in the water each carcass was buoyed up by residual air in the lungs, air entrapped in the fur, and the lowered density of the frozen body tissue, so that the muskrat floated at a level similar to living animals.

All drag measurements were made using a lever type balance (Fig. 2). Six metal bars were positioned orthogonally and welded to a central point. The bars in the rotational axis (Z) acted as a fulcrum and passed through two sets of bearings held in position by brackets. The ends of the bars in the horizontal axis (X) were threaded so balancing weights could be positioned on the bars to align the vertical axis bars at 90° to the protractors (P). The lower bar of the vertical axis (Y) was employed as the mounting bar for the attachment of the experimental animal. At the end of the mounting bar was a plastic bracket (B) shaped as an inverted U.

Figure 2. Drag balance. The three axes are indicated by X, Y, and Z.  $W_b$  represents the counterbalancing weight, B, the mounting bracket used to hold the muskrat and P, the protractors. Procedure for use of the drag balance is given in text.



The ends of the bracket straddled the nose of the muskrat and a large pin was passed through holes in the bracket and into the nose of the muskrat. This arrangement firmly attached the animal to the mounting bar while allowing rotation of the muskrat about the long axis of the pin, but prevented yawing.

When placed in the water current, a torque developed around the rotational axis due to the resistance on the muskrat. The resistance was countered by a sliding weight  $(W_b)$  on the horizontal axis bar. The weight was moved to a point on the bar such that the vertical axis bar was oriented at 90° as determined by siting the vertical axis with the two protractors. The distances from the central fulcrum to  $W_b$   $(1_1)$  and to the pin in B  $(1_0)$  could be measured. The drag on the body of the muskrat was then calculated by the formula:

Drag (N) = 
$$W_b l_1 / l_0$$
 (1)

where  $\mathbf{l}_0$  and  $\mathbf{l}_1$  are measured in meters and  $\mathbf{W}_b$  in kg. Since the mounting bar was not submerged, no correction for drag on the bar was necessary.

The drag of isolated hindfeet was measured in a manner similar to that described above. However, the feet were attached to the mounting bar with a long, narrow screw attached to the end of the bar. The hindeet had been previously frozen in either a fully spread or a fully closed position, similar to the positions of the feet in the power and recovery phases, respectively. The feet were positioned so the plantar surface of the power phase foot and

dorsal surface of the recovery phase foot were normal to the incident water flow. Since the mounting bar was submerged in these tests, the drag on the submerged portion of the bar was subtracted from the foot drag.

Frontal and plantar surface areas of the isolated hindfeet were measured from photocopies of feet using a portable area meter (LAMBDA Instruments Corp. Model LI-3000). The wetted surface area of the body was determined by measuring the length of strings wrapped around the body of a dead, frozen muskrat at 2 cm intervals. This divided the body into numerous small areas which were integrated for muskrats which had been immersed in water to a level approximating a swimming animal.

## Flow Visualization

The water flow around the body of a surface swimming muskrat at 0.3 and 0.6 m/s was observed for a single dead muskrat which was held stationary and parallel to the flow in the water channel. A water soluble ink was injected into the flow around the muskrat through five small diameter tubes (0.7 mm, ID). The tubes were positioned in front of the muskrat and along its sides and posterior end.

## Statistical Procedure

All statistical analyses were made using the statistical programs for a Texas Instruments SR-52 programmable calculator with reference to Simpson et al. (1960) and Steele and Torrie (1960).

In order to perform the statistical analyses for the various data

sets, independence was assumed between trials on living muskrats. Variation about means was expressed as  $\pm$  one standard error (SE), and  $\pm$  S<sub>b</sub> for the regression coefficients.

#### RESULTS

## Metabolic Response

The mean mass-specific oxygen consumption,  $\dot{v}_{02}$ , for muskrats resting in water at 25°C was 0.88  $\pm$  0.03 cc  $0_2/g/hr$  (n=87). The mean resting  $\dot{v}_{02}$  in this study was found to be 62 percent lower than the value reported for restrained muskrats in water at 25°C (Fish, 1979).

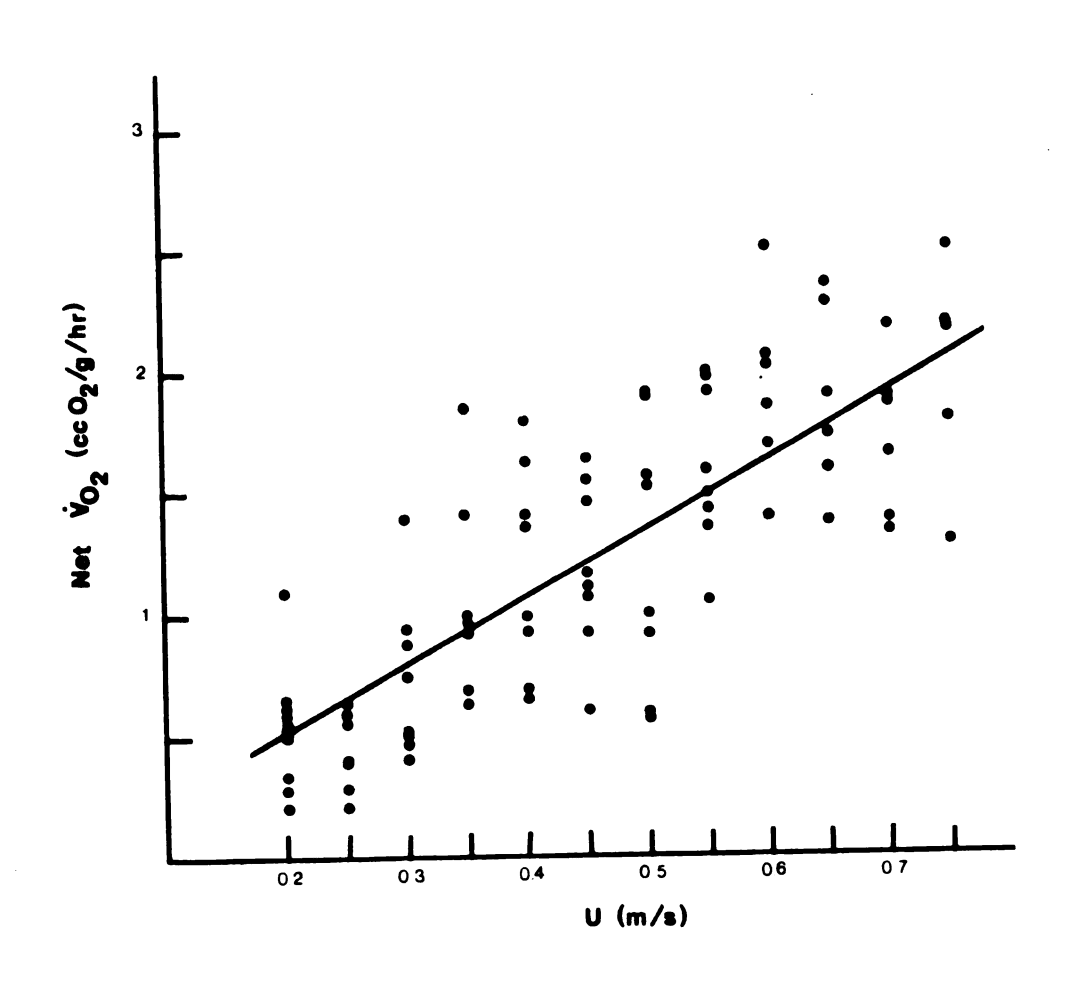
Values of the net  $\dot{v}_{0_2}$  (total - resting) for muskrats swimming in water at 25°C are summarized in Fig. 3. The net  $\dot{v}_{0_2}$  increased linearly as the swimming velocity, U, increased from 0.2 to 0.75 m/s. The equations for the relationships between net and total  $\dot{v}_{0_2}$  and U for all muskrats (n=87) as determined by the best fitting line are given in Table 1A,B.

At velocities of 0.7 and 0.75 m/s several animals were observed to fatigue after 20 min of sustained swimming, as shown by the inability of muskrats to swim against the current. As a result the animals could no longer prevent contact with the downstream electric grid.

## Temperature Effects

Four muskrats were tested at all swimming velocities in water at 25°C and 30°C to determine the effect of ambient temperature on exercise metabolism.

Figure 3. Net mass-specific oxygen consumption of swimming muskrats as a function of swimming velocity, U.



Regressions for metabolic rates of muskrats swimming at various velocities, U, and at different water temperatures,  $\mathbf{T}_{\mathbf{a}}\text{-}$ Table 1.

Metabolic	T,	Velocity	$\dot{v}_0 = aU + b$	aU + b		Correlation
kate	(၁ <sub>၉</sub> )	Range (m/s)	a a	þ	u	Coefficient
A Total	25	0.2 - 0.75	2.60	+0•63	87	0.71**
B Net	25	0.2 - 0.75	2.81 2.81	-0.05	87	0.78**
C Total	25	0.2 - 0.75	2. 52	69.0+	48	**62.0
D Net	25	0.2 - 0.75	3.12	-0.32	84	0.84**
E Total	30	0.2 - 0.75	2.14	+0.70	48	0.75**
F Net	30	0.2 - 0.75	2.22	-0.11	48	0.78**

\*\* - highly significant at P < 0.001

The mean resting  $\dot{v}_0$  s for muskrats in water at 25 and 30°C were 0.86  $\pm$  0.04 (n=36) and 0.77  $\pm$  0.04 cc 0<sub>2</sub>/g/hr (n=40), respectively. The difference between the resting rates was found to be significant at P < 0.001 with a paired t-test at 23 degrees of freedom.

Fig. 4 illustrates the relationship between net  $\dot{V}_{0_2}$  and velocity, U, for muskrats swimming in ambient water temperatures of 25 and 30°C. At both temperatures, the net  $\dot{V}_{0_2}$  increased linearly with increasing U. The equations for the linear regressions for total and net  $\dot{V}_{0_2}$  at both 25 and 30°C (n=48) are listed in Table 1C,D,E,F. All regresions were found to be significant at P < 0.001. The slopes of the total and net  $\dot{V}_{0_2}$  were found to be greater at 25°C than 30°C at P < 0.025 and P < 0.0005, respectively, with a t-test of the regression coefficients at 92 degrees of freedom. The total and net  $\dot{V}_{0_2}$  were higher at 25°C than 30°C, except for net  $\dot{V}_{0_2}$  values for muskrats swimming below 0.23 m/s.

## Body Drag

The drag experienced by the body of the muskrat over the range of U used by living animals is shown in Fig. 5. The drag increased exponentially with increasing U. This is expressed by the equation:

$$Drag = 0.46 U^{1.48}$$
 (2)

The correlation coefficient was found to be 0.9 (n=7), which was

Figure 4. Mass-specific oxygen consumption, Net  $\dot{v}_{0}_{2}$ , as a function of swimming velocity, U, for muskrats in water temperatures of 25 ( $\bullet$ —) and 30 ( $\bullet$ ----) °C.

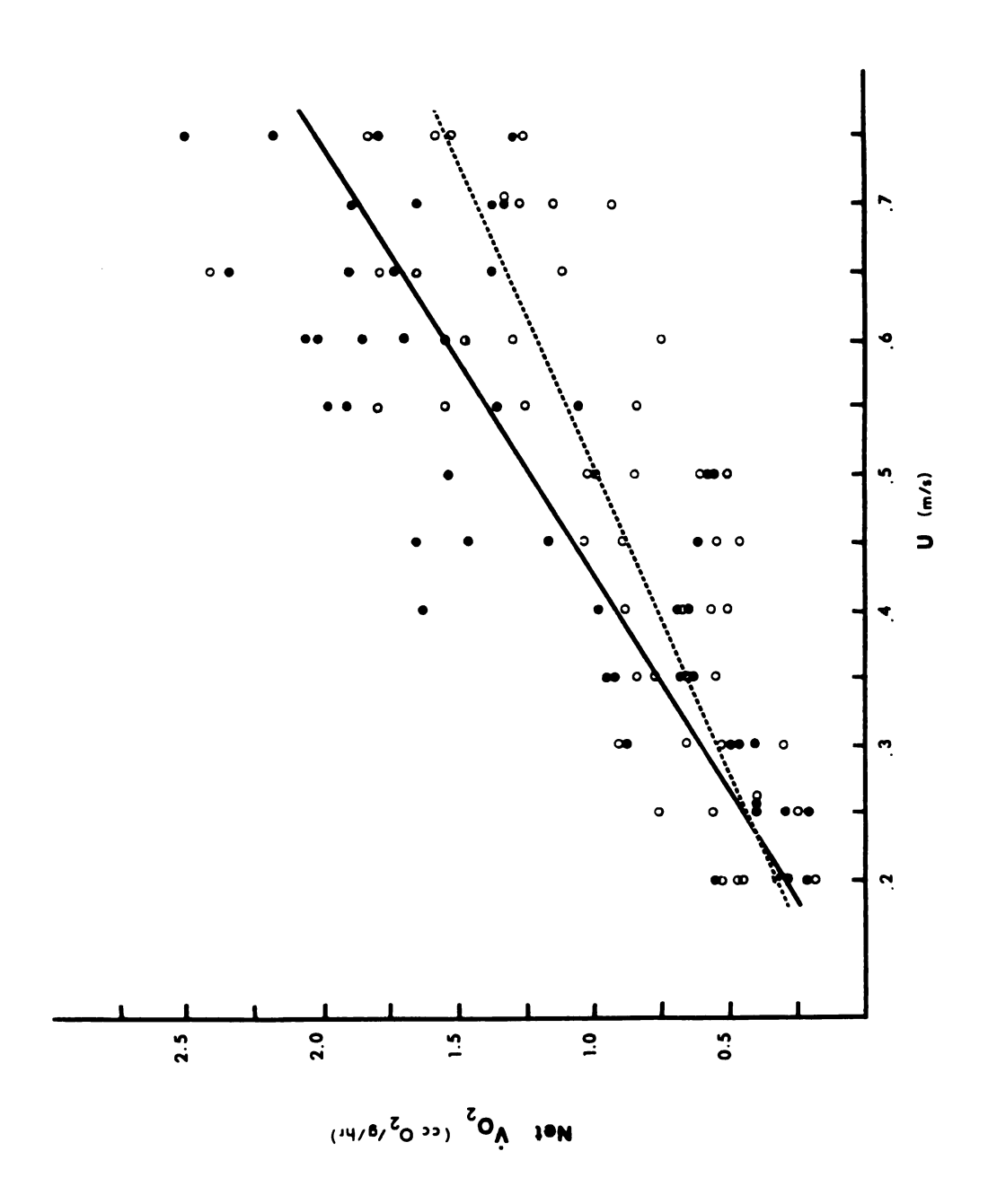
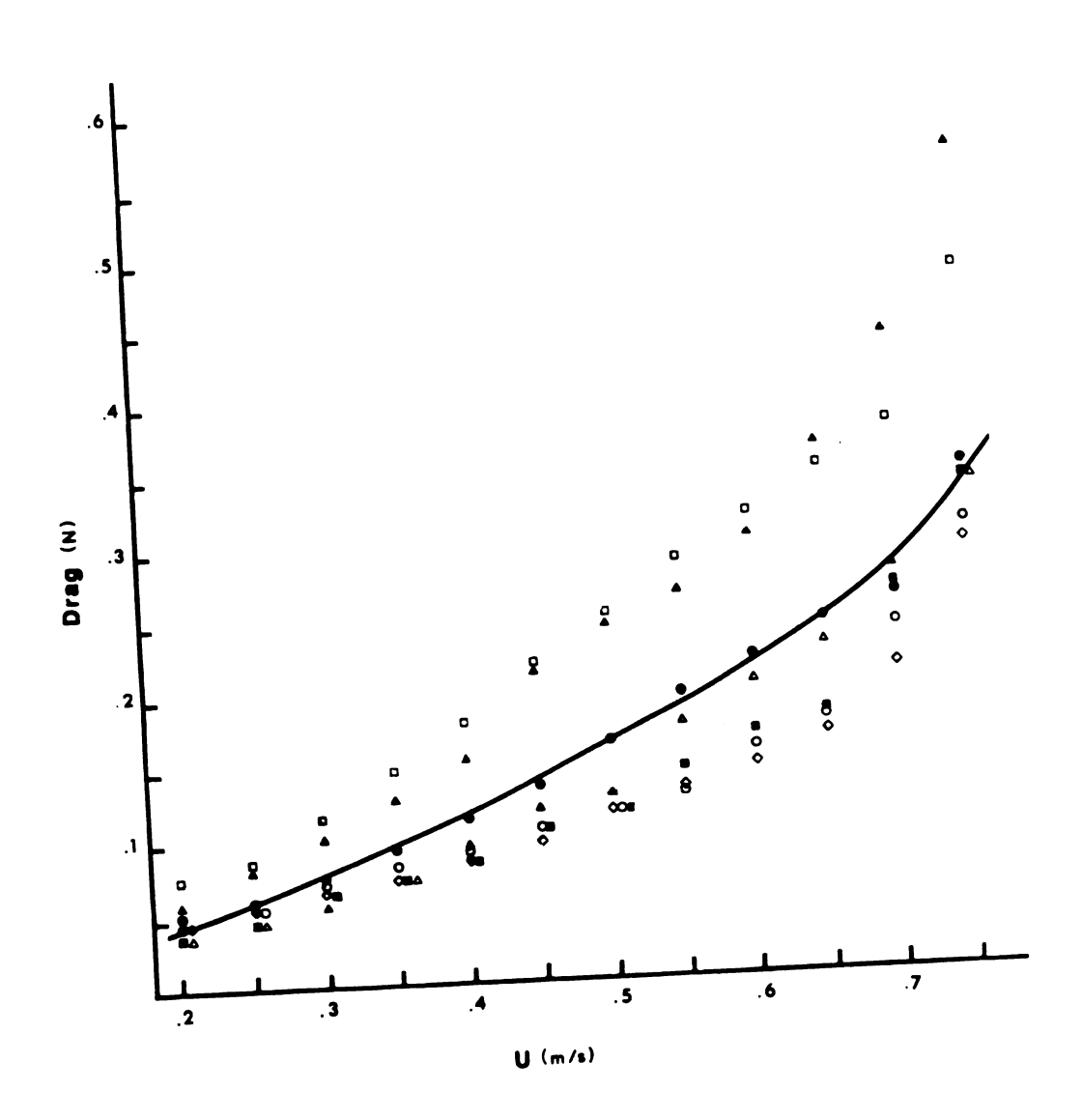


Figure 5. Drag as a function of water velocity, U.

The regression line is given in the text by equation (2). Symbols indicate drag for individual muskrats.



significant at P < 0.001.

## Biomechanics

Kinematics were analyzed on muskrats swimming steadily at velocities from 0.25 to 0.75 m/s. At 0.2 m/s, the experimental animals did not swim steadily. Instead, they accelerated toward the front of the metabolic chamber and then drifted back in the current toward the downstream end. Although this motion was sufficient for metabolic determinations, motion analysis was confined to steady swimming by the animals.

In its normal surface swimming posture, the muskrat maintains a concavely arched back, with the head and pelvic regions being the highest points of the body above the water line (Eble, 1954/55). However, some muskrats were observed to flex their backs, although this was never observed in animals swimming unrestricted in large ponds. The forelegs of the muskrat were held under the chin with the feet flexed, so that the plantar surfaces were held dorsally under the forearm. Short pawing motions were sometimes observed, but were highly irregular. I believe these motions did not contribute to the generation of thrust.

Films of swimming muskrats confirmed the observation of others (Howell, 1930; Kirkwood, 1931; Svihla and Svihla, 1931; Mizelle, 1935; Dagg and Windsor, 1972) that the hindfeet move in a paddling mode. Robinson (1975) has defined paddling as the movement of a paddle antero-posteriorly in a vertical plane parallel to the direction of motion of the craft. For the muskrat, the paddling mode is facilitated by alternating strokes of the hindfeet.

The paddling cycle of the muskrat consisted of power and recovery phases (Fig. 6). The angular velocity of the hindfoot over the time of the stroke cycle shows a sine wave form (Fig. 7).

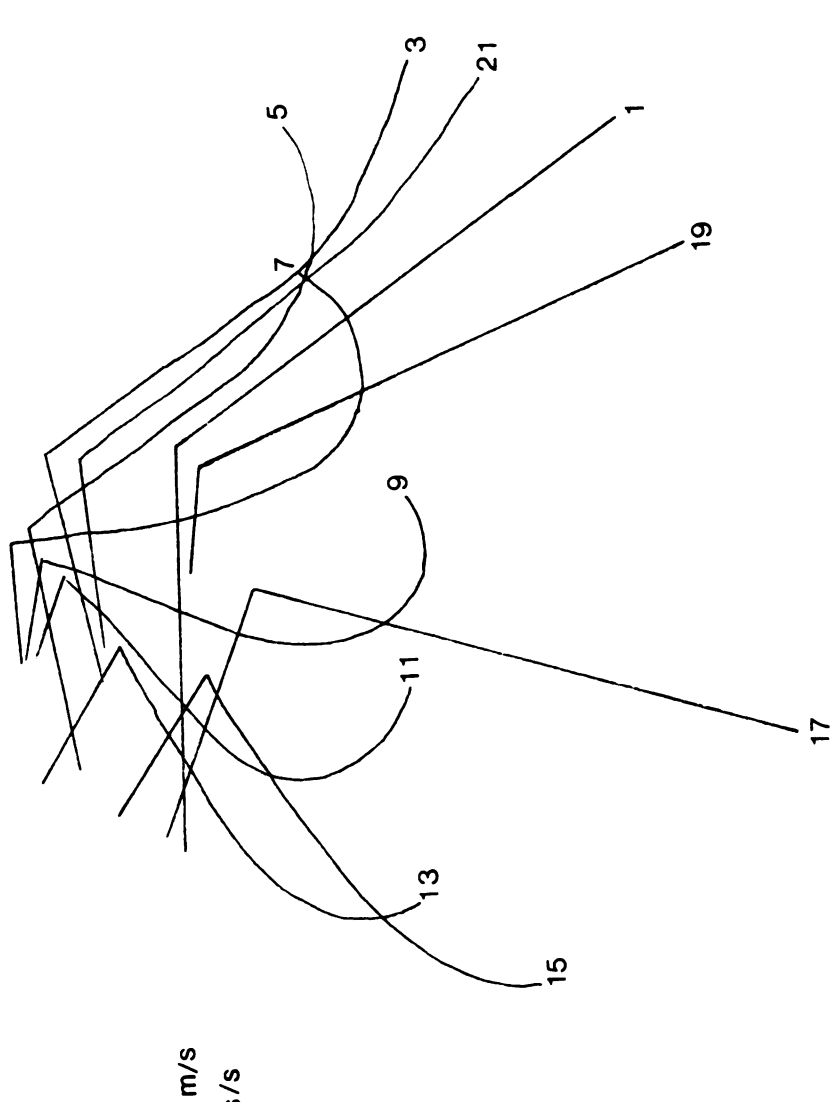
During the power phase (Fig. 6; frames 15-21), the hindfoot was accelerated posteriorly through an arc by plantarflexion of the foot, flexion of the shank, and retraction of the femur. Although the major paddling movements occurred at the ankle joint, movement of the femur showed that retraction of the femur may increase the posterior velocity of the foot by as much as 0.18 m/s. The hindfoot reached a maximum velocity when oriented at an angle of approximately 90° to the horizontal. At the end of the power phase, rapid deceleration of the hindfoot approximates the rate of the acceleration at the beginning of the phase (Fig. 7).

Also during the power phase, the digits were extended and maximally abducted so that they were fully spread and the foot was slightly pronated. Although there is only a slight webbing between the bases of the digits, It appears that the lateral fringe of stiff hairs, each 3-7 mm long, located along the side of each digit is passively erected by the resistance of the water as the foot is swept back. The effective plantar surface area including fringe hairs (mean: 15.74 cm<sup>2</sup>; n=7) was 21 percent higher than the same feet in which the fringe hairs have been removed (mean; 12.46 cm<sup>2</sup>; n=7).

The recovery phase of the stroke cycle (Fig.6; frames 5-13) is characterized by dorsiflexion and supination of the hindfoot, flexion of the digits, protraction of the femur, and extension of the shank. The angular velocity of the foot during the recovery

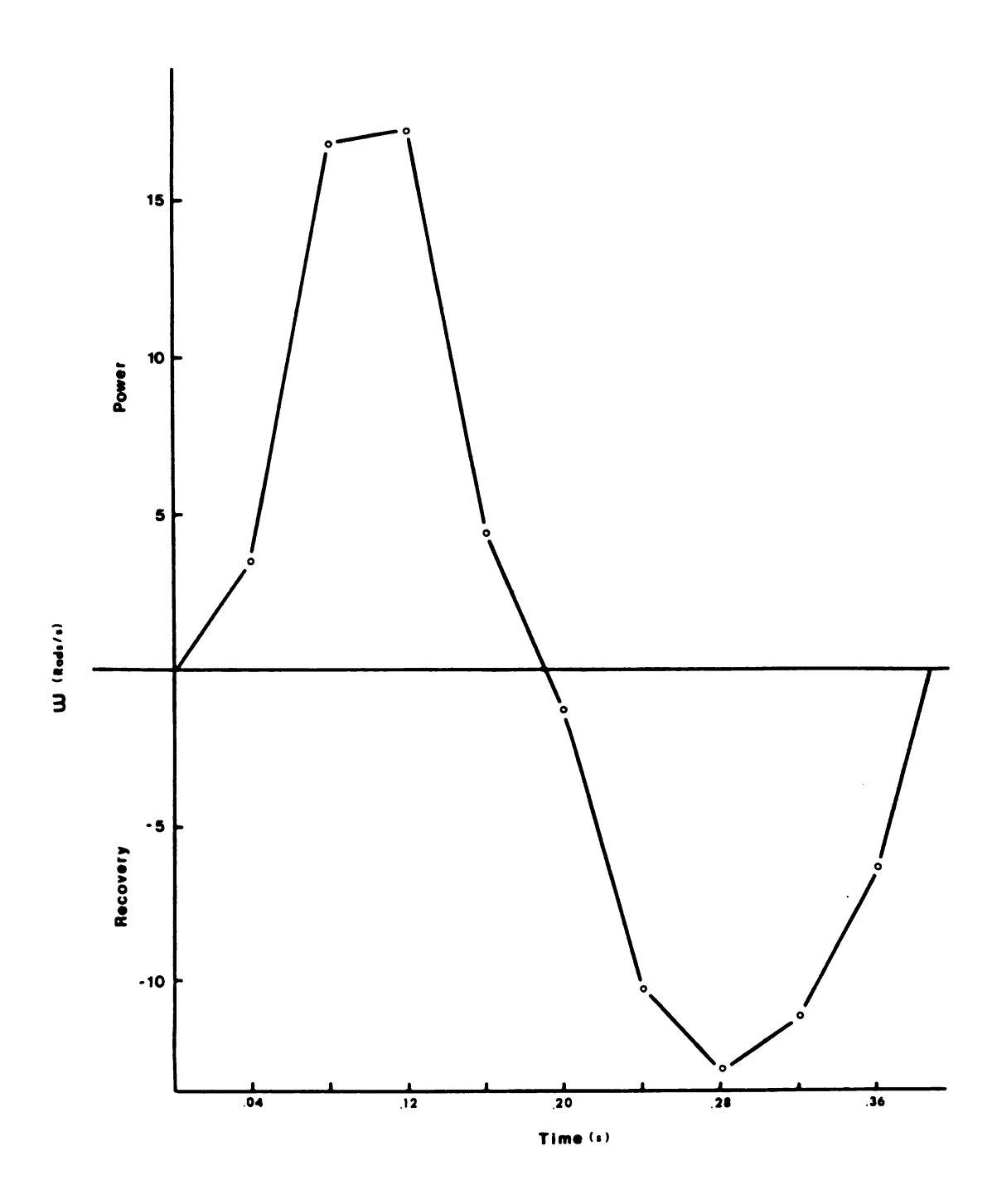
Figure 6. Diagrammatic representation of the lateral view of the hindfoot through the stroke cycle. The alternate sequential frames are indicated by the numbers for each foot position, where the power phase is indicated by frames 15-21 and the recovery phase by frames 5-13.

The segments of the foot shown are the phalanges, metatarsals, tarsals, and tibia.



U - 0.45 m/s 50 frames/s

Figure 7. The angular velocity ( $\omega$ ) of the power and recovery phases of the hindfoot as plotted over the time of one stroke cycle for a muskrat swimming at 0.45 m/s.



phase showed an acceleration to a maximum at 90° to the long axis of the body and then a deceleration of the foot at the end of the phase (Fig. 7). The maximum angular velocity of the recovery phase was on the average 9 percent lower than that of the power phase.

The frontal surface area of the hindfoot during the recovery phase for 7 feet was reduced to a mean value of 7.12 cm<sup>2</sup> by adduction and flexion of the digits and supination of the foot. A similar motion has been observed in grebes (Peterson, 1968).

Fig. 8 illustrates the frequency of the stroke with respect to U. The frequency remains relatively constant over all velocities at  $2.5 \pm 0.06$  Hz. This was similar to the constant stroke frequency seen in swimming ducks (Prange and Schmidt-Nielsen, 1970) and competitive human swimmers (Nadel, 1977). However, this differs from previous observations on the muskrat, beaver, nutria, and mink (Mordvinov, 1976), sea lion (Kruse, 1975), and fish (Bainbridge, 1958; Hunter and Zweifel, 1971), in which the frequency of the propulsive appendages increased with swimming speed. The stroke cycle of the muskrat was asymmetrical in time. The mean durations of the power ( $t_p$ ) and recovery ( $t_r$ ) phases were  $0.18 \pm 0.01$  and  $0.22 \pm 0.01$  s, respectively, over the range of U. The duration of the power phase was found to be significantly shorter than the recovery phase at P < 0.0005 with a paired t-test and 28 degrees of freedom.

The arc through which the hindfeet were swept during the propulsive phase is shown as a function of the swimming velocity of the muskrat in Fig. 9. The arc was determined by measuring the angle made by the metatarsals to the horizontal plane. The arc

Figure 8. The stroke frequency of the hindfeet as a function of the swimming velocity, U.

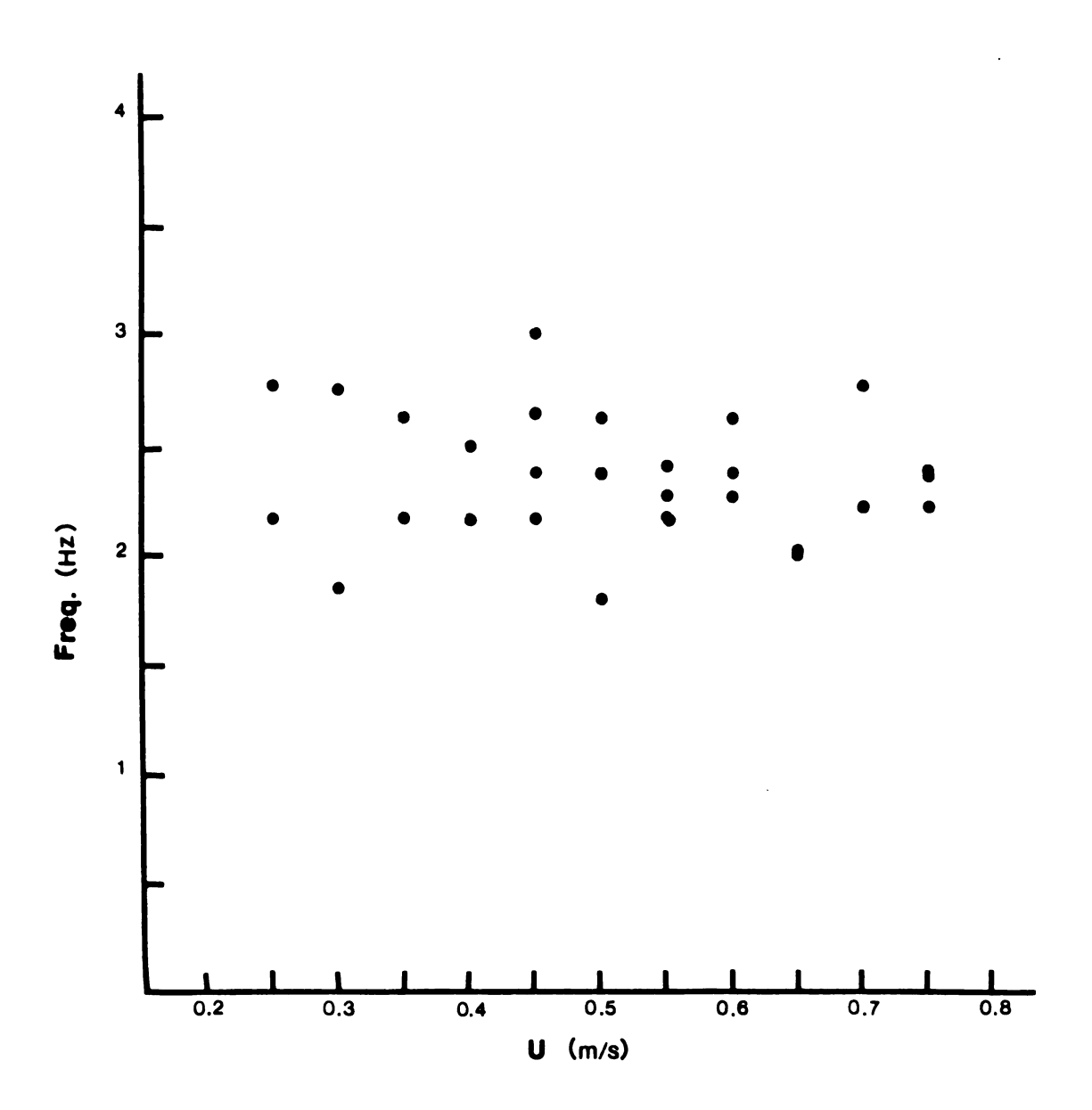
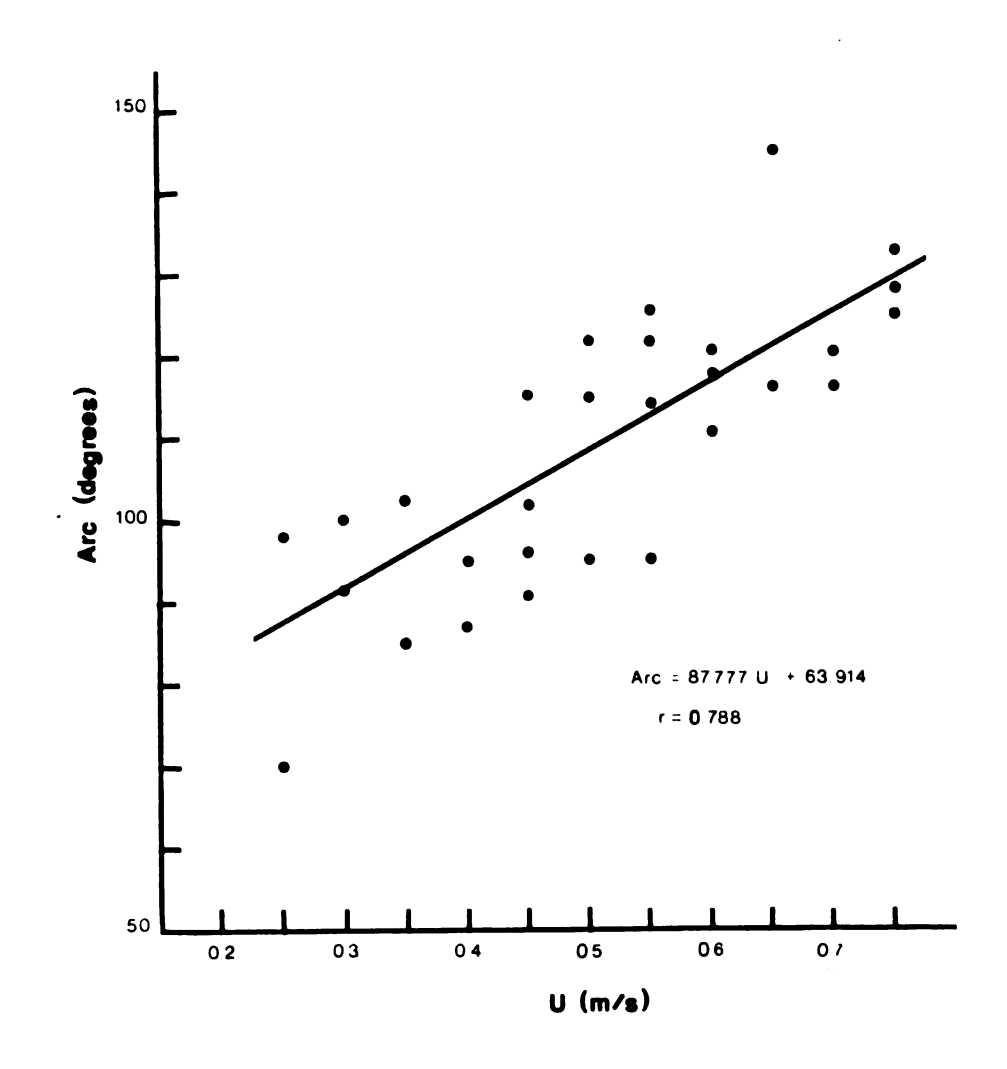


Figure 9. The arc of the hindfoot plotted as a function of the swimming velocity, U.



Likewise, an apparently linear increase with swimming velocity, U, was found to occur for the angle that the hindfoot makes with respect to the long axis of the body at the end of the power phase (Fig. 10). However, the angle assumed by the foot at the start of the power phase remained relatively constant from 0.25 to 0.55 m/s. From 0.6 to 0.75 m/s, the angle of the foot at the start of the power phase showed a hyperbolic relationship, which decreased to a minimum level at 0.65 m/s (Fig. 10).

The importance of the increased surface area from the fringe hairs is illustrated in Fig. 11. At the same water flow velocities, u, the normal force which was measured on the drag balance for an isolated hindfoot with the fringe hairs intact  $(F_p)$  was 20 percent higher than without the hairs  $(F_p')$ . During the recovery phase, the configuration change of the hindfoot represented a reduction of 55 percent from the frontal surface area of the hindfoot (including the fringe hairs) during the power phase. As a consequence of the reduced frontal surface area, the drag for the recovery phase of the hindfoot  $(F_R)$  represents only 33 percent of the drag experienced by a foot in the power phase position  $(F_P)$  (Fig. 11).

In the present study, lateral undulations of the tail were observed, as exemplified in Fig. 12 for a muskrat swimming at 0.5 m/s. Travelling waves were found to move posteriorly down the tail at a velocity faster than U. Amplitude increased along the tail reaching a maximum at the tip. At least one-half to one full wavelength was observed in the tail. These travelling waves were analogous to the tail and body motions seen in anguilliform fish

Figure 10. The angle of the hindfoot to the long axis of the body at the beginning (O) and end (•) of the power phase.

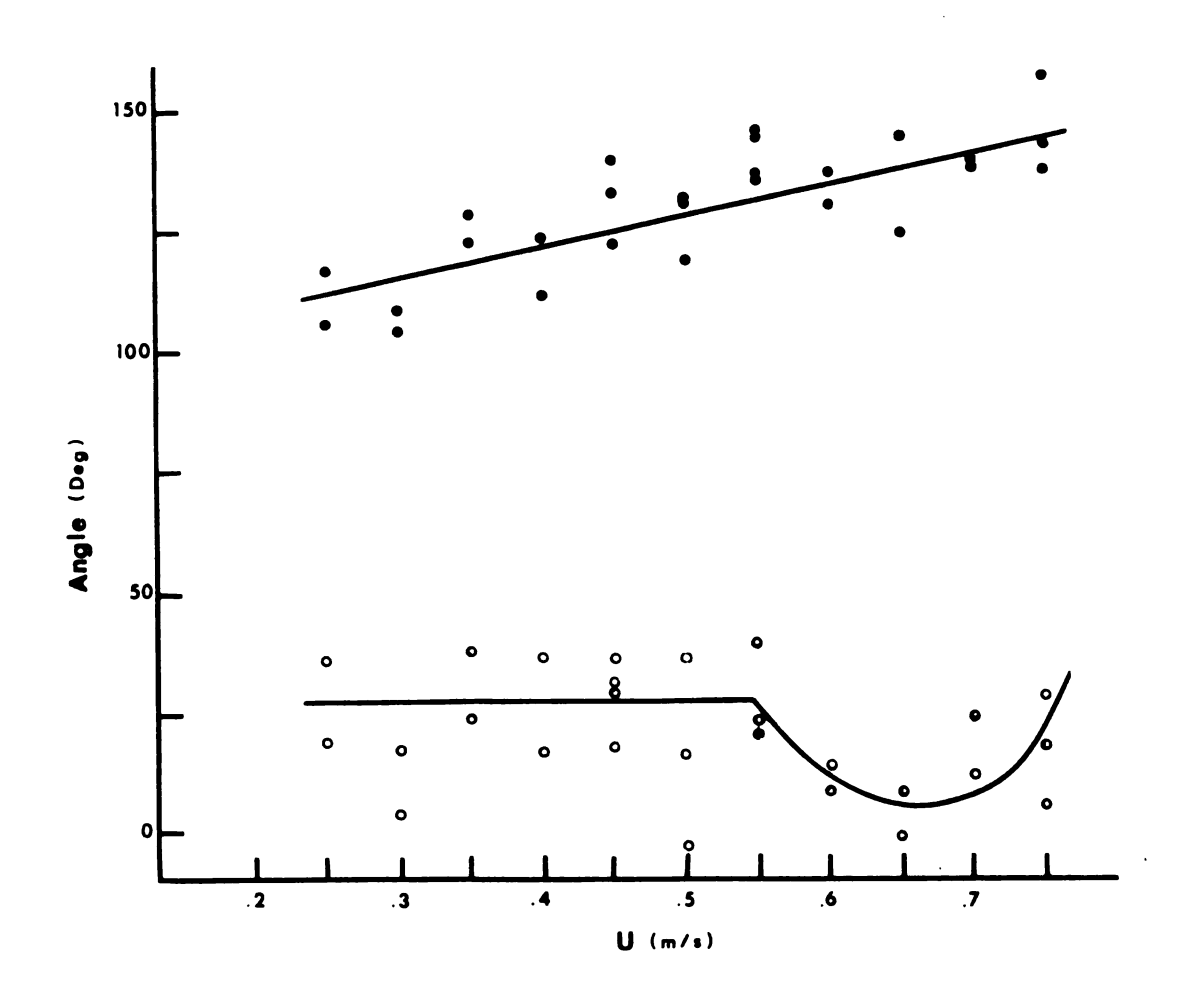


Figure 11. The force on isolated hindfeet determined by drag measurements in the power phase  $(F_p)$ , power phase with fringe hairs removed  $(F_p)$ , and recovery phase  $(F_R)$  as plotted against the water flow velocity, u.

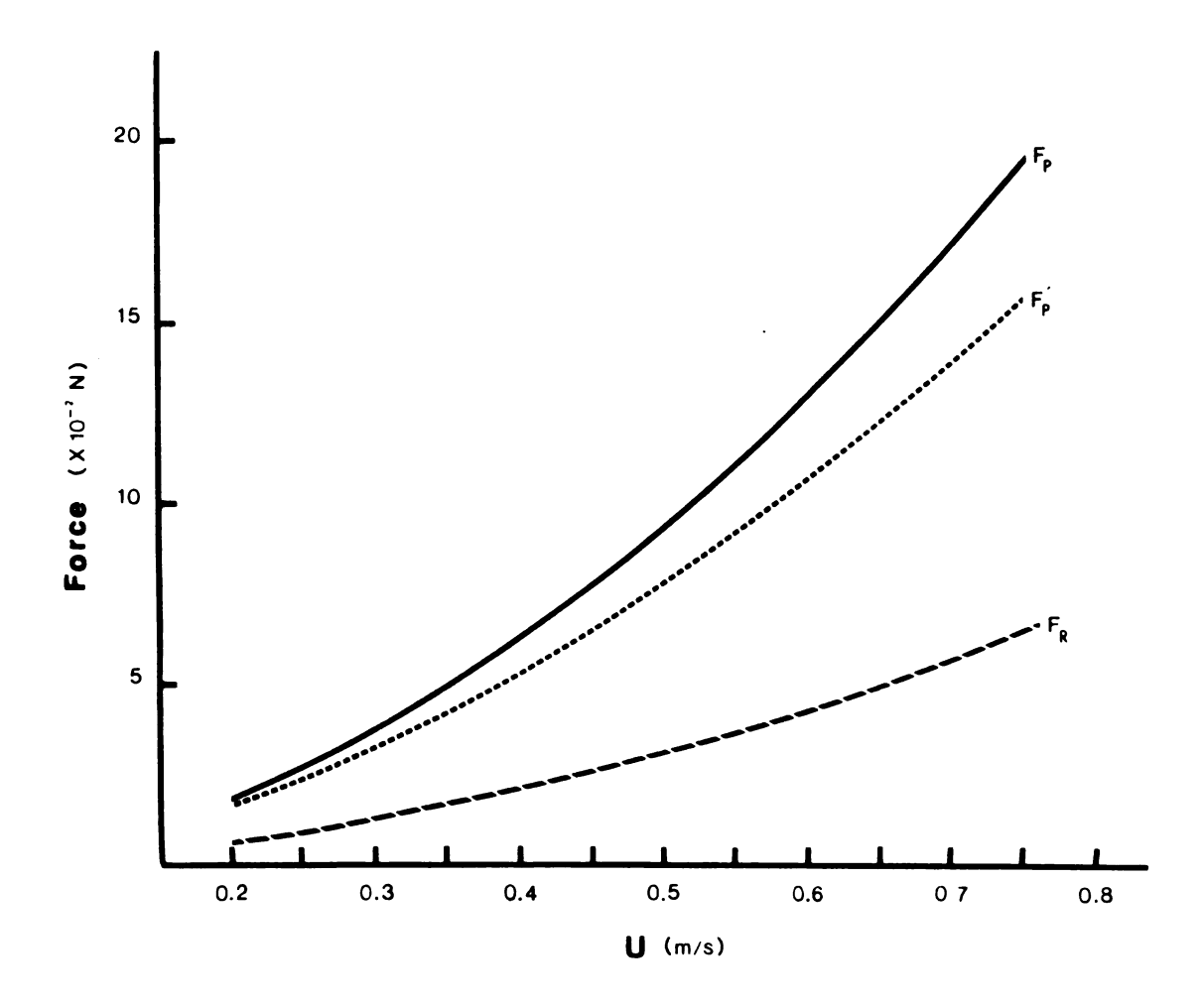


Figure 12. Sequential tracings of the tail of a complete propulsive cycle for a muskrat swimming at 0.5 m/s.

Frames of film are indicated for each tail position.

swimming (Breder, 1926).

The motion of the tail appeared to be synchronized with the hindfoot stroke. The base of the tail was swept to the side opposite the hindfoot which was moving posteriorly initiating the power phase. The frequency of the generation of travelling waves, therefore, remained constant over the range of test velocities at a level of  $2.35 \pm 0.05$  Hz, which was close to the hindfoot stroke frequency. However, a significant difference (P < 0.001) with a paired t-test and 28 degrees of freedom, was found between the two frequencies. This difference was probably due to the independent estimation of both frequencies from film analysis for each trial.

The amplitude of the tail increased linearly with increasing U (Fig. 13), expressed by the equation:

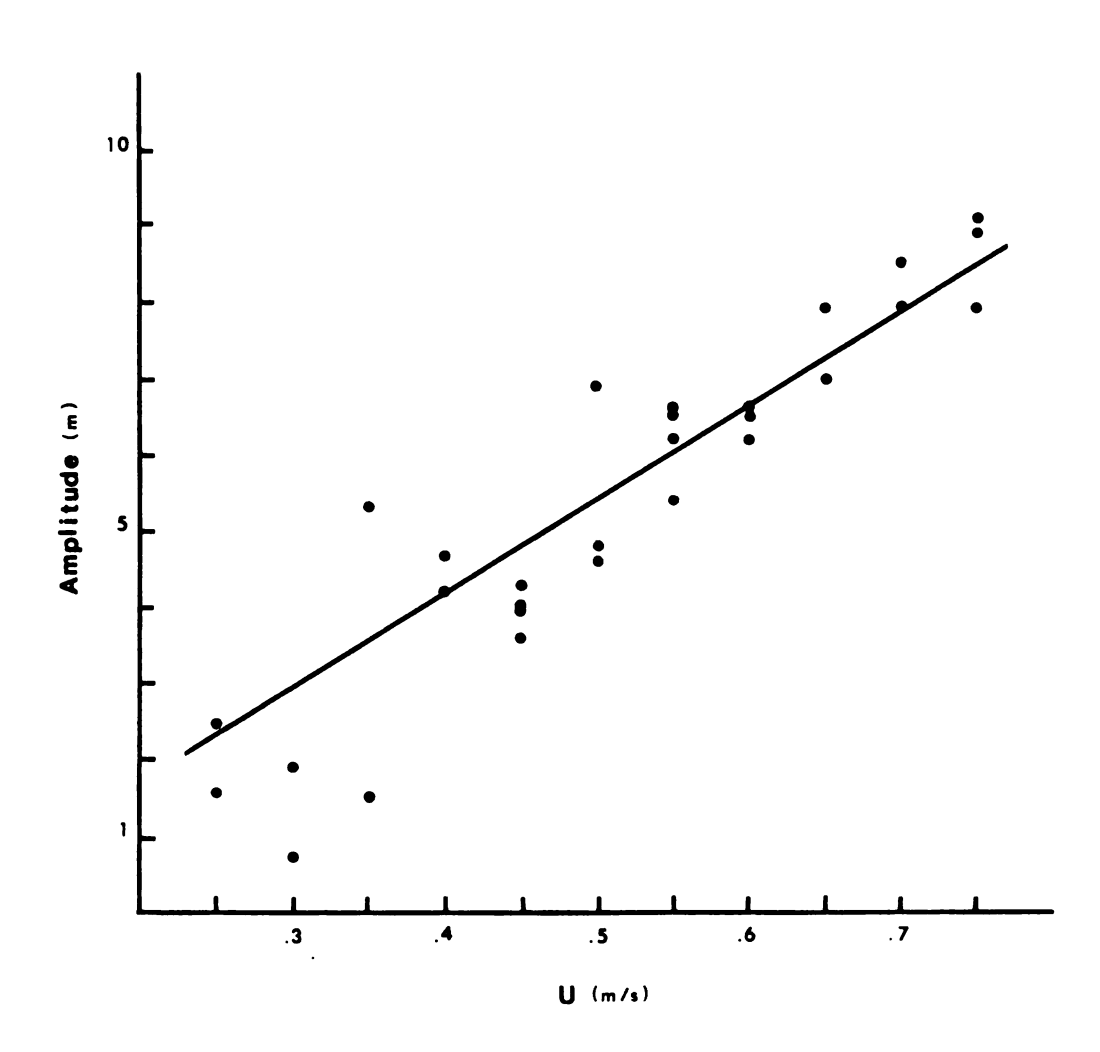
Amplitude = 
$$12.19U - 0.66$$
 (3)

where the amplitude was computed in cm and U in m/s. The regression plotted from the equation with a correlation coefficient of 0.85 was highly significant (P < 0.001). This relationship differs from fish, where the amplitude is constant with increasing swimming velocity (Hunter and Zweifel, 1971).

# Flow Visualization

Ink injected into the water flow just anterior to the muskrat accumulated under the nose, indicating a large stagnation point with a high pressure (Potter and Foss, 1975). The presence of a bow wave anterior to the muskrat indicated the same phenomenon.

Figure 13. Plot of the amplitude at the tip of the tail as a function of the swimming velocity, U.



Much of the ink was swept under the body and encountered large turbulence due to the flow separation which occurred posterior to the deepest part of the body at swimming speeds greater than  $0.6\,$  m/s.

Turbulence along the side of the muskrat was observed at water velocities of both 0.3 and 0.6 m/s. Turbulence with the development of vortices occurred approximately midway down the body of the animal.

The greatest turbulence shown by the ink injection appeared just downstream of the posterior end of the body of the muskrat at all velocities tested. Similar data have been gathered previously on live muskrats by Mordvinov (1974). The turbulence observed allowed water to flow across the tail to the other side of the animal. Both in the region of the tail and farther downstream, the wake of the muskrat showed a considerable amount of turbulence and vorticity.

The water flow about the hindfoot in the power phase showed a large amount of turbulence directly downstream of the foot.

Similar results were also observed for feet positioned in the recovery phase.

#### **DISCUSSION**

# Swimming Energetics

The majority of studies concerned with the energetics of swimming locomotion have studied fish which use the sub-carangiform mode (see review by Webb, 1975a). Only recently have there been investigations that dealt with the energetic input necessary for alternate modes of swimming by fish ( $e \cdot g \cdot$ , Webb 1975a, b; Gordon et al., 1979). Very few examinations of surface swimming have been attempted. Ducks, which swim by a paddling stroke similar to that of the muskrat, maintain a relatively constant oxygen consumption below 0.5 m/s (Prange and Schmidt-Nielsen, 1970). Over the range of swimming velocities from 0.5 to 0.7 m/s, ducks exhibited an exponential increase in metabolic rate. This differs from the response by the muskrat where  $\dot{v}_{0}$  increases in a linear manner up Humans (Nadel et al., 1974) and marine iguanas to 0.75 m/s. (Gleeson, 1979) also showed a linear increase of metabolic rate with increasing swimming velocity. However, sea lions and sea turtles, which have a low profile in the water and use a hydrofoil type propulsor (Walker, 1971; Robinson, 1975; English, 1976), both exhibited exponential increases in metabolic rate with increasing velocity (Kruse, 1975; Prange, 1976).

Although the relationship between  $\dot{v}_{02}$  and U for swimming

Although the relationship between  $\dot{V}_{O_2}$  and U for swimming muskrats is best explained statistically by a linear curve, some individuals tended to show a limit in their  $\dot{V}_{O_2}$  between 0.6 and 0.75 m/s at a level approximately 3 times the resting  $\dot{V}_{O_2}$ . These data, along with observations of fatigue in several animals at 0.7 and 0.75 m/s, and fastest speed of 0.84 m/s for muskrats swimming in controlled experiments (Mordvinov, 1977) suggests that the muskrat has reached a limit in its aerobic capacity at the higher velocities. Increased power input to generate thrust may therefore come from a large anaerobic component of the total metabolism.

Such an initiation of anaerobic metabolism in swimming vertebrates has been previously documented. Brett (1964) showed that salmon swimming above 4 body lengths/s peak in their aerobic metabolism and go into oxygen debt. Webb (1971b) believed that moderate activity such as cruising in trout was not associated with any significant level of anaerobic metabolism. However, when velocities of the trout reached 80 percent of the critical speed, he felt that the anaerobic energy to comprised a significant amount of the total energy expenditure. Swimming horses showed a linear increase of oxygen consumption with increasing work effort; however, they demonstrated no plateau in  $\hat{V}_{02}$ , even though they utilized a large anaerobic component (Thomas et al., in press).

Terrestrial locomotion by young lions has demonstrated a linear increase of oxygen consumption to a plateau with increasing running speed (Chassin et al., 1976). Tests on inclines supported the contention that the plateau was the maximum aerobic capacity.

Blood lactate measurements on the running lions at submaximal levels showed an increase with increasing speed.

In the muskrat, small amounts of lactic acid are probably accumulated in the body at submaximal levels. Ruben and Battalia (1979) found that in small rodents anaerobiosis accounted for one-third of the total energy expended in the first 30 sec of maximal activity. This is most likely due to the lag of the circulatory system in providing oxygen and nutrients to active tissue at the initiation of activity by the animal (DiPrampero et al., 1970). Webb (1971b) suggested that anaerobic metabolism is utilized in the first few minutes of a new activity level in trout.

Although there is a possible contribution by anaerobic metabolism to the power input at a U above 0.6 m/s, and because studies of the lactic acid levels of muskrat tissues during exercise have not been completed, further discussion of the energetics of muskrat swimming will be confined to all velocities tested.

The difference between the maximum  $\dot{V}_{0}$  and the resting  $\dot{V}_{0}$  (aerobic scope of activity) for the muskrat in water at 25°C was found to be 2.00 cc  $0_2/g/hr$ . The maximum aerobic energetic expenditure, expressed as its ratio of the resting  $\dot{V}_{0}$ , was found to be only 3.3 for the swimming muskrat. This is at the lower part of the range of aerobic scope values for small mammals (Wunder, 1970), and far below the values for humans and dogs (Pasquis et al., 1970). The predicted maximum  $\dot{V}_{0}$  for the muskrat can be determined using the equation of Pasquis et al. (1970):

$$\max_{0} v_{0}(\cos v_2/\min) = 0.436M_b (g)^{0.73}$$
 (4)

The calculated value (4.92 cc  $^{0}2/\text{min}$ ) is 41 percent higher than the observed limit in  $\dot{v}_{0}$  .

Prange and Schmide-Nielsen (1970) have argued that the lower maximum  $\dot{V}_{0_2}$  for swimming ducks when compared to flying birds was due to the difference in the percentage of muscle utilized in each activity. However, this explanation for the small metabolic scope is unlikely in the case of the muskrat as Hart (1971, p. 116) stated that "in no rodent has it been possible to produce by exercise an increase in metabolism exceeding the peak level in the cold." Maximum metabolic rates for muskrats exposed to a range of ambient air temperatures were 3.3 (Hart, 1962) and 2.7 times (McEwan et al., 1974) the resting rate. Therefore, even if all the muscles besides the swimming muscles were exercised, the metabolic scope of the muskrat would not be expected to increase.

## Temperature Effects

For the muskrat, a semi-aquatic, endothermic homeotherm, the energetic expenditure for swimming may be profoundly influenced by the ambient water temperature in conjunction with swimming speed.

This would be due in part to the high thermal conductivity of water.

Muskrats exhibited a significant difference in  $v_{0}$  between water temperatures of 25 and 30°C over the entire range of swimming velocities. This is different from results obtained for humans swimming at submaximal levels in water at 17.4, 26.8 and 33.1°C

°C (Costill et al., 1967). It was found that for humans, the energy requirements for swimming were not significantly affected by water temperature, although effects were observed on core body temperature and heart rate during recovery. However, Nadel et al., (1974) found that the cost of swimming at different water speeds and temperatures was greatest at the lower water temperature tested of  $18^{\circ}$ C. Pasquis et al. (1970) found that for acclimated white mice, white rats, golden hamsters, and guinea pigs the highest values of  $v_{02}$  were obtained in experiments at a low temperature.

The  $V_{0_2}$  may be dependent on the endogenous heat load of the body. In examining the body temperature of Merriam's chipmunk, Wunder (1970) found that body temperature was dependent on running speed at an ambient temperature of 35°C. Fish (1979) has shown that while resting in 30°C, water muskrats acquired a large internal heat load, raising body temperature to a mean of 39°C before vasomotor mechanisms were activated. Muskrats swimming in the summer show an elevation of body temperature believed due to the rise in metabolic heat production which is not compensated for by a decrease in thermal insulation (MacArthur, 1979). The muskrat is not able to withstand high ambient temperatures (McEwan et al., 1974), which result in a high body temperature (Johansen, 1962b; Fish, 1979). The in  $V_{0_2}$  may therefore be affected by the interaction of ambient temperature, body temperature, heat production, activity state, and thermal conductance of the animal through heat convection. In respect to the thermal conductance, although the conductivity of water is high, convective heat loss at differing water temperatures and U may remain the same due to turbulence from swimming motions, which distorts the flow around the body (Nadel et al., 1974). In humans at 18°C, the higher  $\dot{v}_{02}$  with increasing U compared to 26 and 33°C water temperature were believed due to increased metabolism for thermoregulatory needs supplied by shivering (Nadel et al., 1974).

The slopes for the relationship between  $V_{02}$  and U at 25 and 30°C were found to be significantly different. For muskrats, the  $\dot{V}_0$  at 25°C was higher than at 30°C. Mount and Willmont (1967) 2 found the opposite situation in that for active white mice, where the increase in oxygen consumption was less at 8 and 15°C than at 23°C. Such results are contrary to Hart (1971) who stated that rodents performing equal levels of activity increase oxygen consumption by equal amounts, independent of environmental temperature.

The difference in the regressions of  $V_{O_2}$  and U for muskrats at 25 and 30°C water temperature is likely due in part to the convective effect of the velocity of the medium, since all turbulence generating movements were confined to the wake of the muskrat. Gessamen (1972) found that for the snowy owl (Nyctea scandiaca) at any air temperature the metabolic rate was a function of the ambient temperature and square root of the wind velocity. A similar relationship has been found for other birds (Robinson et al., 1976; Chappell, 1980a), but measurements on the pelage of mammals shows a direct relationship between the convection coefficient and wind velocity (Chappell, 1980b).

# Drag and Power Output

A body moving through a fluid medium experiences a force which resists forward motion. This resistance force is commonly known as drag. The drag is composed of frictional, pressure, and gravitational components.

The frictional component is due to the viscosity of the flow about a body in the boundary layer, producing a shear force. The pressure component is also due to viscosity, but results from pressure differentials along the body. The pressure difference results in separation of the boundary layer from the body, producing vorticity in the outer flow. Finally, the gravitational component is due to the production of waves at the water surface. The waves produced by a body moving on the water suface are generated through the loss of kinetic energy by the body (Prandtl and Tietjens, 1934). The major cost of propulsion for ships is the energy lost in the production of surface waves (Schmidt-Nielsen, 1972a). For submerged swimming, the drag is dominated by frictional and pressure components. The total drag is proportional to the square of the velocity for a totally submerged body at a high Reynolds number (Potter and Foss, 1975). In comparison, the drag experienced during surface swimming has frictional, pressure, and gravitational components. Because of the complex drag force at the air-water interface, there exists no predictive equation for surface swimming; so that the drag must be determined empirically.

For the muskrat the dominant components of drag are pressure and gravitational. The former component was demonsteated by flow visualization around the body of the muskrat with the appearance of

visualization around the body of the muskrat with the appearance of vortices along the posterior one-half of the body and in the wake. The formation of vortices was due to boundary layer separation along the body due to an adverse pressure gradient (Webb, 1975a). The observed vorticity represented energy lost from the muskrat to the water as pressure drag.

Correspondingly, production of surface waves by the muskrat was indicative of a loss of kinetic energy to the water. In deep, unbounded water, a body, such as a ship, in motion on the surface is accompanied by two sets of waves (Prandtl and Tietjens, 1934); (1) the "diverging waves" which move off the bow and stern at an angle of 40° from the central axis, and (2) the "cross waves" in which the crests are oriented perpendicular to the direction of motion.

The "diverging waves" dominate the drag produced by wave formation. This is due to the interference between the diverging waves off the bow and stern which is dependent on the wave length and velocity of the body. The relationship between the wavelength (L) and velocity (U) is expressed as:

$$U = \sqrt{gL/2} \tag{5}$$

where g is the gravitational acceleration of  $9.8 \text{ m/s}^2$  (Prange and Schmidt-Nielsen, 1970).

As velocity of the body is increased, the bow and stern waves constructively interfere with each other, so that the body is situated in a wave trough, dramatically increasing drag (Prange and

Schmidt-Nielsen, 1970). This condition arises when the wavelength equals the waterline length of the body. At this time the body is then said to have reached its "hull speed."

Prange and Schmidt-Nielsen (1970) have utilized the concept of hull speed to interpret swimming in ducks. They found the predicted hull speed to occur at the maximum sustained swimming velocity. Rapid increase in oxygen consumption of the duck as hull speed was approached was believed to be in response to the increased drag due to wave interference.

A mean waterline length of 0.25 m was measured on dead muskrats which were partially immersed in water. From this a hull speed of 0.63 m/s was calculated for the muskrat. This was surprisingly similar to the velocity above which swimming muskrats showed fatigue. The advent of increased energetic demands by anaerobiosis at high velocities may be in response to the large surface drag as hull speed is attained.

For the muskrat, drag was related to the velocity raised to the 1.48 power. Since the muskrat is a surface swimming animal and subject to the gravitational forces, the body drag experienced by the animal cannot be expected to conform to the relationship absent of a free surface.

Measurements of the drag force experienced on surface swimming animals have only been performed previously on ducks (Prange and Schmidt-Nielsen, 1970), sea turtles (Prange, 1976), and humans (Clarys, 1979), all of which have shown large drags. Although the drag on dolphins and whales has been estimated hydrodynamically (Gray, 1936; Kermack, 1948; Parry, 1949; Lang, 1975), these

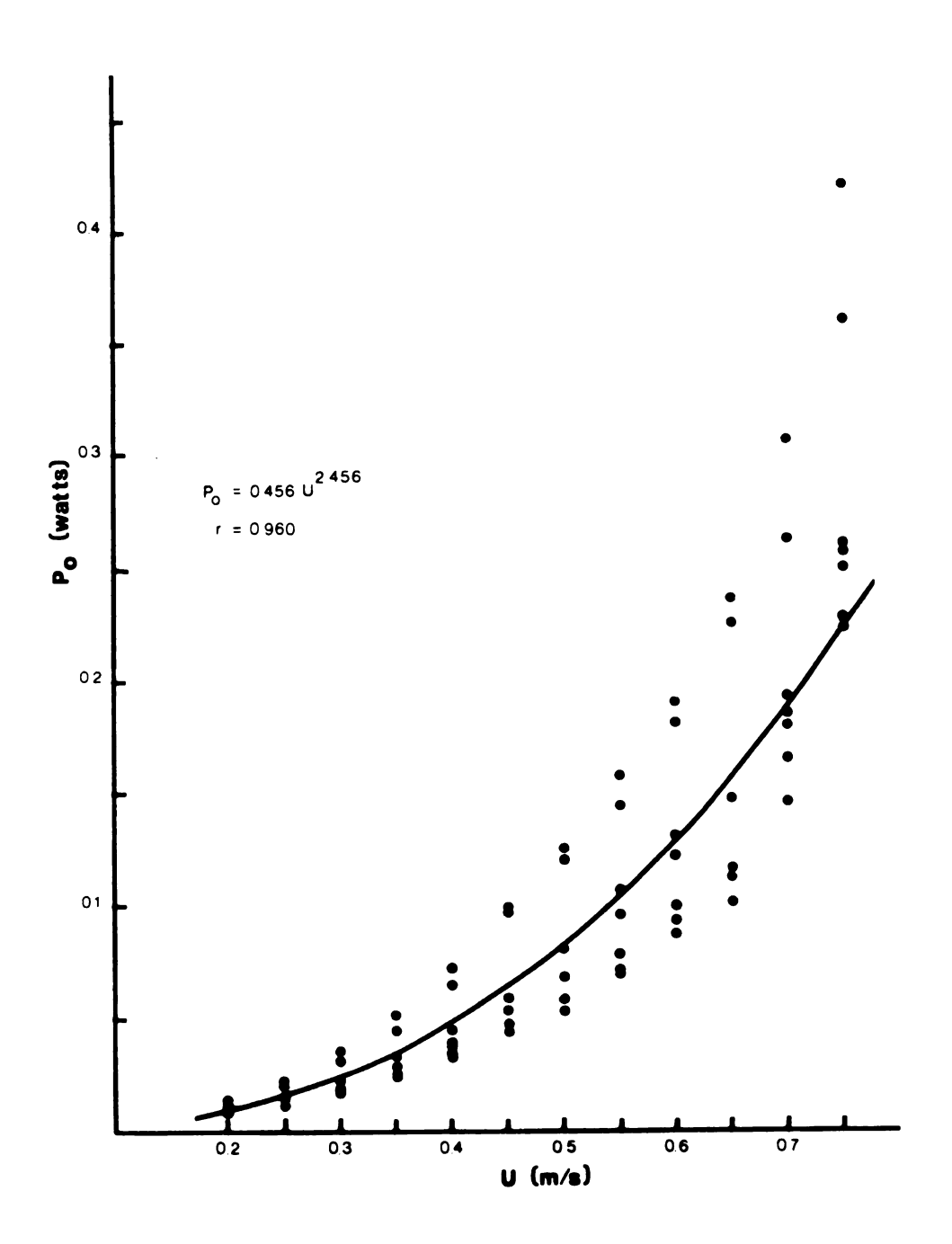
have been assumed for an animal which was totally submerged with no interaction at the air-water interface. This does not take into consideration measurements taken by Hertel (1966) which indicated that a dolphin was not independent of surface effects until it was submerged 3 times its maximum body depth.

If a body is moving at a constant velocity, it can be considered to be in a dynamic equilibrium, in which the total sum of all forces on the body equals zero. Thus, the drag on a moving body which is not accelerating is equal in magnitide, but opposite in direction to the thrust. The power output represents the thrust power necessary to move the body at a constant velocity, and can be computed as the product of velocity and drag force.

The drag power output,  $P_0$ , for the muskrat plotted against U is illustrated in Fig. 14.  $P_0$  was found to increase significantly (P < 0.001) at U raised to the 2.46 power.

The maximum  $P_0$  for muskrats swimming at 0.75 m/s was calculated at 0.22 W. This was considerably lower than the maximum  $P_0$  for the dolphin, Lagenorhychus obliquidens (Lang and Daybell, 1963). In comparison to the  $P_0$  of similarly sized fish as summarized by Webb (1975a), the muskrat fell below expected levels. The difference may in part be due to differences in procedure in that measurements on fish were made during accelerations or that only part of the work by the fish was actually measured. Additionally, the dolphin and fish use a relatively greater percentage of the body musculature in swimming compared to the muskrat, and possess highly efficient locomotor appendages.

Figure 14. The drag power output of the muskrat,  $P_{\rm O}$ , as a function of the swimming velocity, U.



## Thrust, Power and Energy

The mechanics of appendicular swimming propulsion in animals have only recently come under scrutiny (Robinson, 1975). The major thrust in research on aquatic locomotion has concerned movement by lateral undulations of the body and median fins (see review by Webb, 1975a).

To describe the forces developed and compute the power consumption and efficiency during paddling, two mathematical models have recently been developed by Alexander (1968) and by Blake (1979, 1980a,b). Both models consider paddling to be a drag-based mechanism of propulsion.

Alexander (1968) used a mechanical analogue (rowboat). The boat is considered to move forward at a constant velocity, U, and experience a drag, D, resisting forward motion. Because the oars during the power stroke move posteriorly relative to the boat, the oar has a resultant velocity, u - U, where u is the velocity of the oar. The drag on the oar in the power stroke is d, so that the power produced by the two oars is 2d(u - U). During the recovery stroke, the direction of the oar is reversed so that the resultant velocity is (u + U) and the power output is 2d'(u + U), where d' is the drag on the recovery oar.

Alexander's model, however, does not adequately describe the paddling or rowing motion observed in animals. Paddling appendages, which have a fixed joint at the body, are swept through an arc so that the resultant velocity and drag are changing through the cycle. Alexander's model appears more relevant to the latter half of the power stroke in the Australian crawl or breaststroke in

human swimmers (Counsilman, 1968; Schliehauf, 1979).

A modification was used to calculate the thrust generated by a muskrat swimming at 0.45 m/s. Integration of the drag on the feet throughout the entire cycle, also taking into account the change in arc, gave values of negative thrust!

blake (1979, 1980a) employed blade-element theory to determine the forces developed on the segments of a pectoral fin of an angelfish (Pterophyllum eimekei) which is a drag-based propulsor. Blake (1980b) assumed that the drag force acting on the appendage was due solely to pressure drag, that the nature of the induced velocity field could be neglected, and that there was no interference between the appendage and the body.

A modification of Blake's model was used to compute the power and energy generated for the paddling appendages of the muskrat. Both the power and recovery phases were analyzed similarly except for the resultant relative velocity of the hindfoot. Unlike the blade-element theory used by Blake, all forces for the whole cycle were estimated from a convenience point on the foot, designated as the center of action  $(C_A)$ , which approximated the point where the mean force would act. For the power phase,  $C_A$  was represented by the distal end of the second metatarsal. When a circle was drawn such that  $C_A$  was in the middle and the radius was determined as the distance from  $C_A$  to the end of the phalanges, 66 percent of the plantar surface area of the foot was enclosed in the circle. Full details of all assumptions used in the model were given by Blake (1979, 1980a,b).

The normal  $(v_n)$  and spanwise  $(v_s)$  components of the paddle

velocity are calculated by:

$$v_0 = Wr - Usin Y \tag{6}$$

$$v_{s} = U\cos Y \tag{7}$$

where  $\omega$  is the angular velocity,  $\gamma$  is the angle between the paddle and the horizontal (Fig. 15), and r is the effective radius of the paddle. The effective radius was estimated by measuring the distance between  $C_A$  and the intersection of lines extrapolated from the metatarsal toward the body. The intersection point fell close to the position of the acetabulum for feet in the power phase. The resultant relative velocity (v) is:

$$v = (\omega^{2}r^{2} + U^{2}\sin^{2}y - 2U\omega r \sin y + U^{2}\cos^{2}y)^{1/2} (8)$$

$$= (\omega^{2}r^{2} + U^{2} - 2U\omega r \sin y)^{1/2}$$
(9)

where v is positive as the paddle moves posteriorly.

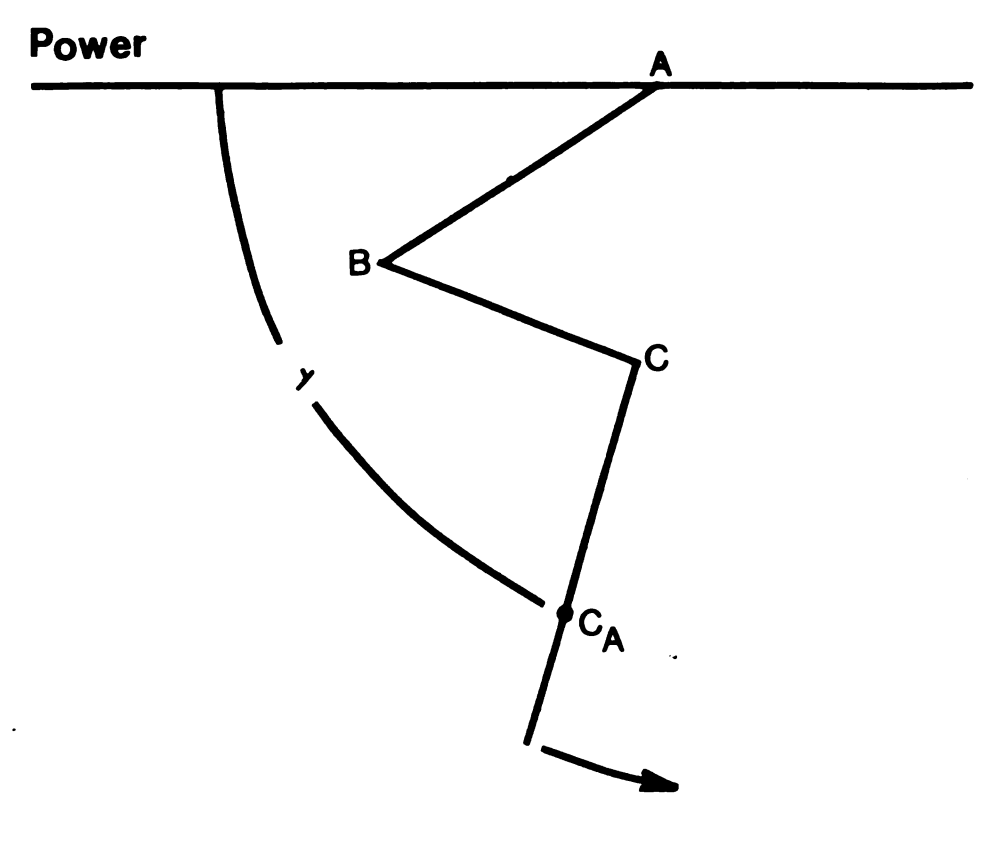
$$\sin^{\alpha}_{a} = v_{n}/v \tag{10}$$

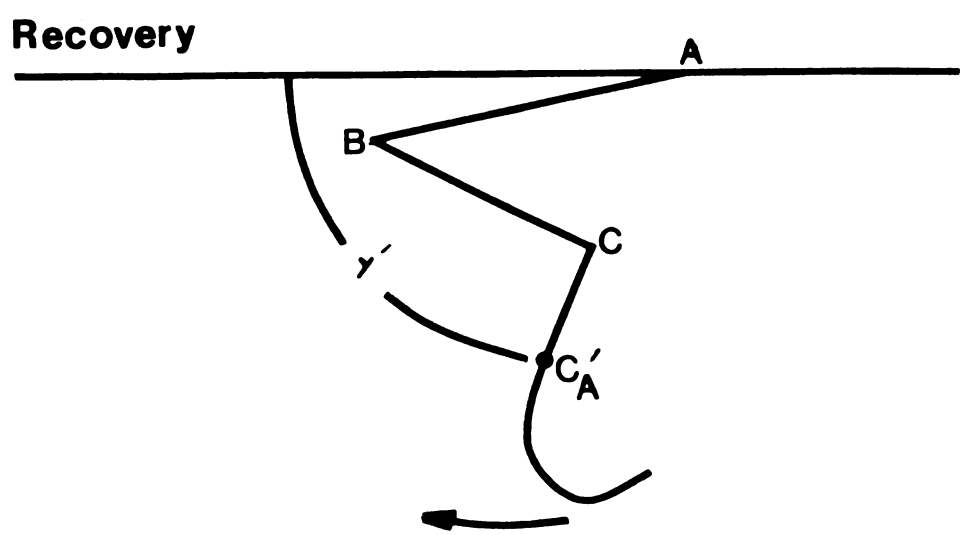
The normal force  $(\mathrm{d}F_n)$  acting at  $C_A$  is due primarily to pressure drag and calculated as:

$$dF_n = 1/2 \rho v^2 AC_n \tag{11}$$

where e is the water density (1000 kg/m<sup>3</sup>), A the area of the

Figure 15. Schematic diagram of the hindfeet during the power and recovery phases showing the orientation angles,  $\gamma$  and  $\gamma$ , and the centers of action,  $C_A$  and  $C_A$ . The acetabular, knee, and ankle joints are represented by A, B, and C, respectively.





paddle plantar surface, and  $C_n$  the normal force coefficient. As explained by Blake (1979),  $C_n$  = 1.1 when  $\alpha_a$  is greater than 40°. Below  $\alpha_a$  = 40°,  $C_n$  decreases linearly so that  $C_n$  can be approximated as:

$$C_n = k \sin^{2} a \tag{12}$$

where k = 2.5.

The component of thrust used for forward propulsion  $(dT_p)$  is:

$$dT_{p} = dF_{n}\sin \gamma \tag{13}$$

The instantaneous rate of working by the paddle  $(dW_p)$  and rate of work done used for thrust  $(dW_t)$  are expressed by:

$$dW_{p} = \omega r dF_{n}$$
 (14)

$$dW_{t} = \omega r dT_{p}$$
 (15)

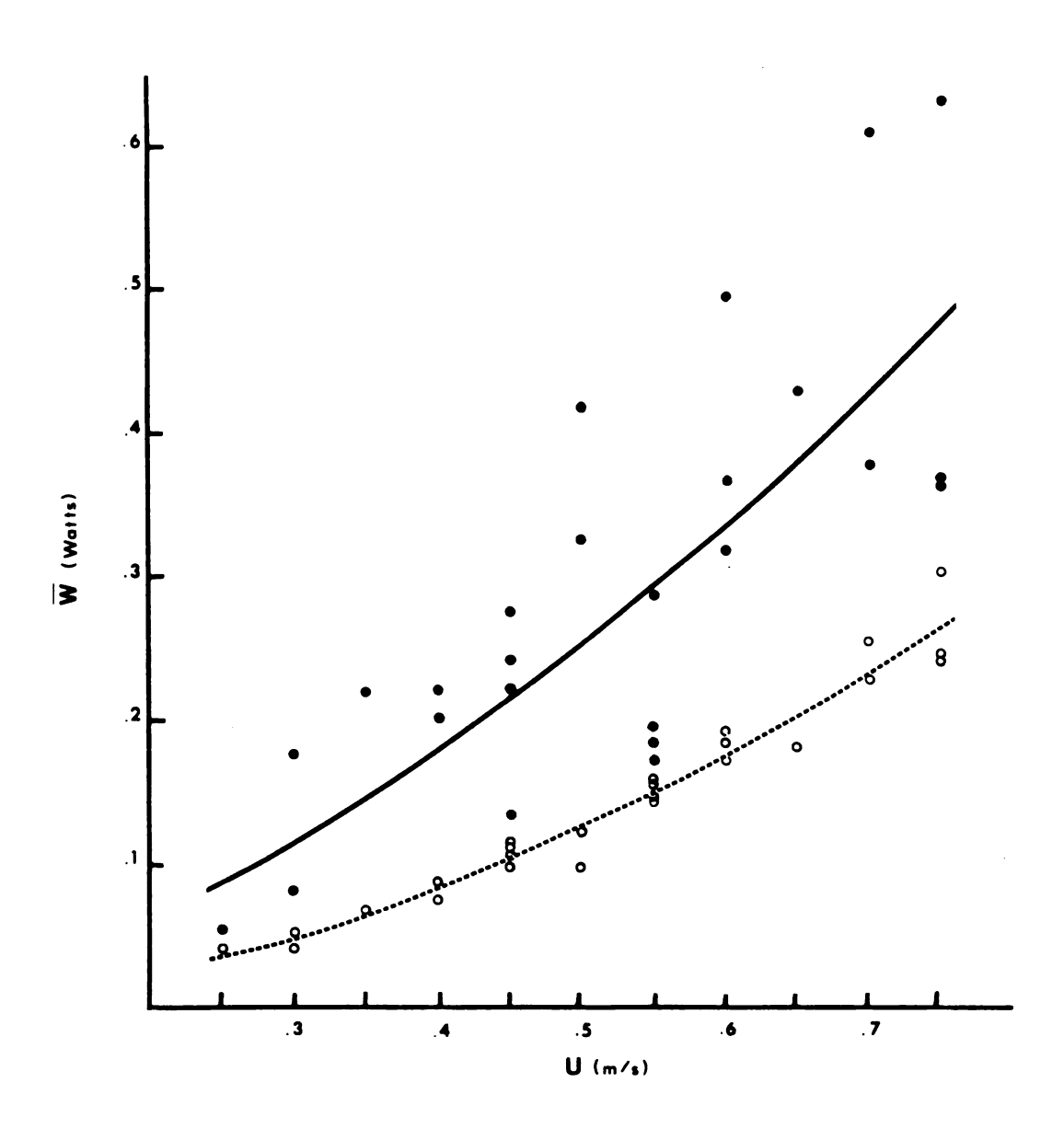
The mean power generated over the power phase and the mean propulsive power generated are:

$$\overline{W}_{p} = 1/t_{p} \int_{0}^{t_{p}} dW_{p} dt$$
 (16)

$$\overline{W}_{t} = 1/t_{p} \int_{0}^{t_{p}} dW_{t} dt$$
 (17)

 $\overline{\textbf{W}}_{p}$  is plotted for each U tested in Fig. 16. The total

Figure 16. The mean power expended during the power (—),  $\overline{W}_P$ , and recovery (—),  $\overline{W}_r$ , phases for one paddle as a function of the swimming velocity, U.



energy (E  $_{\rm p}$ ) and thrust energy (E  $_{\rm T}$ ) expended during the power phase for one paddle are calculated from equations (16) and (17) by excluding  $1/t_{\rm p}$ .

The regression of  $\overline{\boldsymbol{W}}_p$  on  $\boldsymbol{U}$  of the muskrat fits the equation:

$$\overline{W}_{D} = 0.751 U^{1.56}$$
 (18)

which is highly significant (P < 0.001) with a correlation coefficient of 0.821 (n = 25).

The curvilinear increase of propulsive power of the paddling muskrat with increasing U is similar to the power developed by swimming trout as measured by Webb (1971a). Webb also used models by Taylor (1952) and Lighthill (1969, 1970) for calculation of propulsive power of trout and found similar responses to increasing U.

Because of the configuration of the hindfeet during the recovery phase, it was assumed that the drag on the foot should be dominated by the pressure component. Therefore, the recovery phase can be analyzed in a similar manner to the power phase. However, the direction of the foot movement is opposite to the direction of body movement, so that the perpendicular velocity,  $\mathbf{v_n}^{\dagger}$  is:

$$v_n' = \Omega r' + U \sin \gamma' \tag{19}$$

and the spanwise velocity,  $v_s'$ , is:

$$v_{s}' = U\cos\gamma' \tag{20}$$

The radius, r', and orientation angle,  $\gamma$ ', were determined in a similar manner to that in the power phase. However, the digits during the recovery phase were plantarflexed, so that  $C_A$ ' was shifted to a new position estimated as half-way between the rotation point and distal end of the second metatarsal.

The resultant relative velocity of the recovery phase is:

$$v' = (\Omega^2 r'^2 + U^2 + 2U\Omega r' \sin \gamma')^{1/2}$$
 (21)

The normal force  $(dF_n^{\ \ \prime})$  acting at  $C_A^{\ \prime}$  is given by:

$$dF_n' = 1/2ev'^2A'C_n'$$
 (22)

where  $C_n$ ' is determined by the same assumptions as for the power phase and calculated using equations (10) and (12) with values for the recovery phase interjected. The drag on the hindfoot acting in the opposite direction to forward motion is given by:

$$dT_r = dF_n' \sin \gamma' \tag{23}$$

The rate of working during the recovery phase  $(dW_r)$  and rate of working directly opposed to thrust  $(dW_{rt})$  is:

$$dW_{r} = \Omega r' dF_{n}'$$
 (24)

$$dW_{rt} = \Omega r' dT_r$$
 (25)

The mean power utilized  $(\overline{W}r)$  and mean power opposed to forward motion  $(\overline{W}_{rt})$  is expressed by:

$$\overline{W}_{r} = 1/t_{r} \int_{0}^{t_{r}} dW_{r} dt$$

$$\overline{W}_{rt} = 1/t_{r} \int_{0}^{t_{r}} dW_{rt} dt$$
(26)

 $\overline{W}_r$  is illustrated over the range of U in Fig. 16. Similar to  $\overline{W}_p$ ,  $\overline{W}_r$  showed an exponential increase with increasing U, where:

$$\overline{W}_r = 0.444 U^{1.822}$$
 (28)

The correlation coefficient of 0.986 for the regression line was found to be highly significant at P < 0.001 (n = 25).  $\overline{W}_{r}$  represented 41-55 percent of  $\overline{W}_{p}$  over the range of U.

The total energy expended during the recovery phase  $(E_r)$  and energy expended against thrust  $(E_{rt})$  are calculated from equations (26) and (27) by excluding  $1/t_r$  from the equations.

The energy expenditure for power and recovery phases on the limb are given in equations (15) and (23), respectively. In addition, the energy losses required to overcome the inertia and added mass of the hindfoot were calculated.

The energy necessary to move the mass of the hindfoot (Blake, 1979) ( $E_{\rm f}$  for power and  $E_{\rm f}$ ' for recovery phases) is:

$$E_{f} = \int_{0}^{t} 1/2m_{f}v^{2}dt \qquad (29)$$

where t may be the time for either the power or recovery phase and  $m_{\rm f}$  is the mass of the hindfoot which was 9.36 g.

The added mass was assumed to be represented by the mass of water contained within the volume of a cylinder formed from rotation about the long axis of the foot. Therefore, according to Blake (1979) the added mass of the hindfoot for either the power or recovery phase is:

$$m_a = (c/2)^2 1 \rho$$
 (30)

where c is the maximum chord of the foot (power: 0.04 m; recovery: 0.01 m) and 1 is the length of the foot (power: 0.08 m; recovery: 0.03 m). The power required to accelerate and decelerate  $m_a$  during the power or recovery phase is given by:

$$W_{a} = \int_{0}^{t} m_{a} avdt \qquad (31)$$

where a is the acceleration of the hindfoot. The acceleration which is always positive was calculated from the slopes of v and v' plotted against the time of the stroke cycle. The energy expended during the power phase is given as:

$$E_a = W_a t_p \tag{32}$$

and the recovery phase as:

$$E_a' = W_a t_r \tag{33}$$

Since the travelling waves in the tail move posteriorly faster than the muskrat swims and with increasing amplitude toward the tip, it is possible that the muskrat utilizes this appendage to generate additional thrust (Gray, 1933; Lighthill, 1969, 1970). Wu (1971) has suggested that swimming is most efficient as amplitude is increased toward the end of the tail. The production of thrust by sculling movements of the tail in muskrats has been previously hypothesized (Dugmore, 1914; Johnson, 1925). However, these studies have not sought to determine the exact nature of the propulsive wave or compute the thrust force generated.

A simplified bulk momentum version of Lighthill's slender body model (Lighthill, 1969, Webb, 1978) was employed to determine the power produced by the muskrat tail. The mean thrust power of the tail, P<sub>T</sub>, is calculated as:

$$P_{\rm T} = mwUW - 1/2mw^2U \tag{34}$$

where m is the virtual mass per unit length, w is the relative velocity of the tail, and W is the tail trailing edge lateral velocity.

The virtual mass per unit length, m, is given as:

$$m = k_T \rho (d_T^2/4)$$
 (35)

where  $k_T$  is a constant equal to 1.0 (Lighthill, 1970),  $\rho$  is the

density of water, and  $d_T$  if the maximum depth of the tail. From specimens used in this study, a mean value of m was computed as 0.212 kg/m. This value is probably a slight over-estimate due to the tapering effect of the tail.

The relative velocity of the tail was calculated from:

$$w = W(V - U/V) \tag{36}$$

where V is the backward velocity of the propulsive wave. The values for w should only be evaluated as an approximation, since the water velocity, U experienced by the tail was probably modified by the turbulence in the wake of the body and hindfeet. The mean values for each wave parameter at each U are presented in Table 2. As with the paddling foot stroke, the frequency of tail flexion remained constant as tail amplitude increased linearly over the range of U. This is opposite to the situation seen in fish swimming at high velocities (Bainbridge, 1958).

Fig. 17 illustrates the relationship between  $P_{\rm T}$  and U.  $P_{\rm T}$  was found to increase curvilinearly with increasing U where:

$$P_{\rm T} = 0.013U^{3.011} \tag{37}$$

which was significant at P < 0.001 with a correlation coefficient of 0.893.

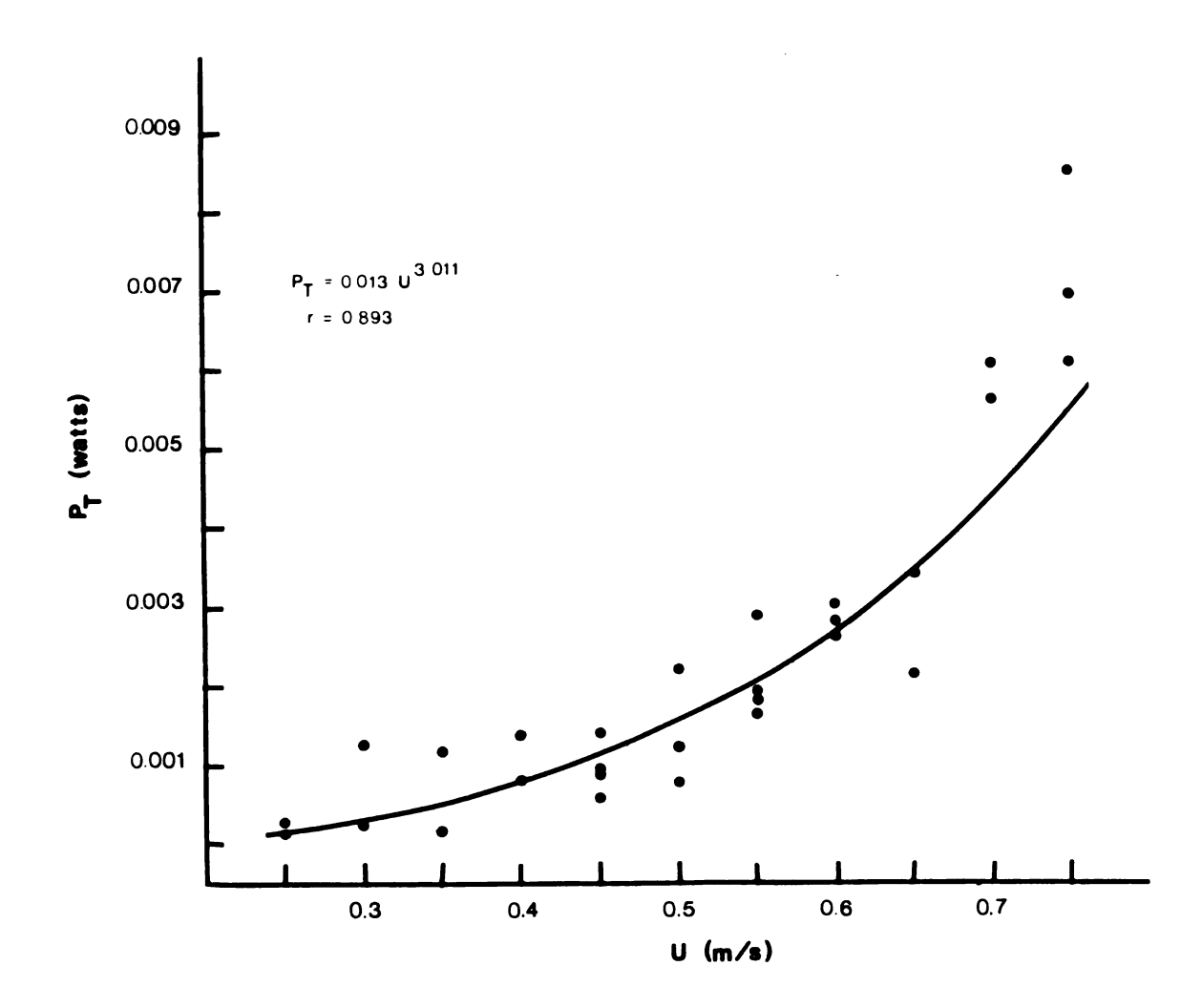
The net energy necessary to generate thrust by the muskrat over the entire propulsive cycle is:

6. 75 5.05 10. 85 10. 85 9. 58 1. 67 4. 28 4. 28 20. 50 2. 86 1. 07

2.15

(m/s) (m/s) (m/s) 0.11 0.01 0.01 0.02 0.02 0.02 0.02 0.03 0.03 0.03 0.04 0.04 0.02 0.04 0.04 0.02 0.04 3 Amplitude Mean tail wave parameters. 0.021 0.005 0.075 0.005 0.034 0.019 0.045 0.001 0.040 0.062 0.003 0.064 0.001 0.075 0.004 0.054 0.005 0.081 (E) Frequency (cycles/s) 2. (s/m) Table + SE 0.45 + SE 0.5 + SE 0.55 + SE 0.65 0.25 + SE 0.3 + SE + SE + SE 0.35 + SE 0.65 + SE 0.7

Figure 17. The thrust power generated by the tail,  $P_{\rm T}$ , as a function of the swimming velocity, U.



$$E_{th} = 2(E_T - E_{rt}) + P_T t_0$$
 (38)

where the energy expended by the foot is multiplied by 2 to take account of both hindfeet. Empirically,  $E_{\mbox{th}}$  was found to correspond to the following:

$$E_{th} = 0.31U^{2.31} \tag{39}$$

which was significant at P < 0.001 with a correlation coefficient of 0.68 and n = 25.

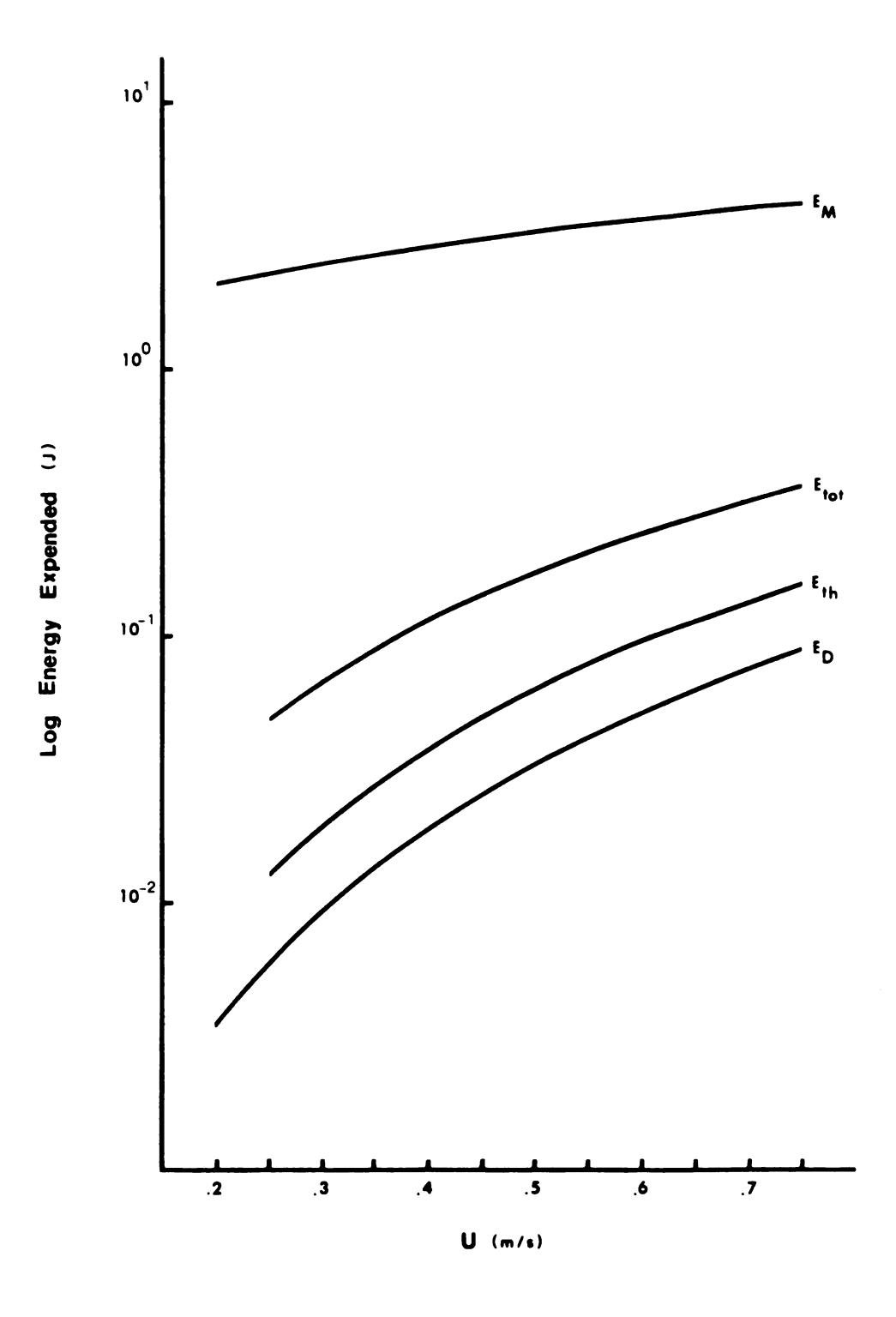
The regression of  $E_{th}$  on U is illustrated in Fig. 18. In comparison to the line for the propulsive energy expended based on drag ( $E_D$ ) calculated from the product of  $P_O$  and  $t_O$ , and also shown in Fig. 18,  $E_{th}$  is 1.8-2.0 times greater than  $E_D$  over the range of test velocities which is small in terms of the variability in the determination  $E_{th}$ . Such a difference between these two independently derived measures is probably due to the movements of the propulsive appendages and acceleration of the body which were not taken account of in the estimation of  $E_D$ . This has also been a primary problem preventing correspondence between similar measures in fish (Webb, 1975a).

## Efficiency and Cost of Transport

The metabolic thrust efficiency,  $\eta_{aerob}$ , for the swimming muskrat was computed by:

$$\eta_{\text{aerob}} = E_{\text{th}}/E_{\text{M}}$$
(40)

Figure 18. Comparison of the logs of energies (E $_{
m M}$ , E $_{
m tot}$ , E $_{
m th}$ , E $_{
m D}$ ) expended at various swimming velocities, U.



where  $E_M$  is calculated from the regression equation for the total metabolic rate at 25°C in Table 1A multiplied by the mean mass of the muskrats, caloric conversion factor of 4.8 cal/ccO<sub>2</sub>, t<sub>o</sub> and 4.185 to convert the metabolic energy to Joules.  $E_M$  is illustrated against U in Fig. 18.  $E_{th}$  was calculated from Eq. (39). The aerob was found to increase steadily to a measured peak value of 0.025 at 0.6 m/s (Fig. 19).

The overall energetic efficiency,  $\eta_e$ , was calculated as the ratio of the sum of the energies expended during the stroke to the metabolic energy and is given by:

$$\gamma_e = E_{tot}/E_M \tag{41}$$

E<sub>tot</sub> is computed by:

$$E_{tot} = 2(E_p + E_f + E_a + E_r + E_f' + E_a') + mwUWt_o$$
 (42)

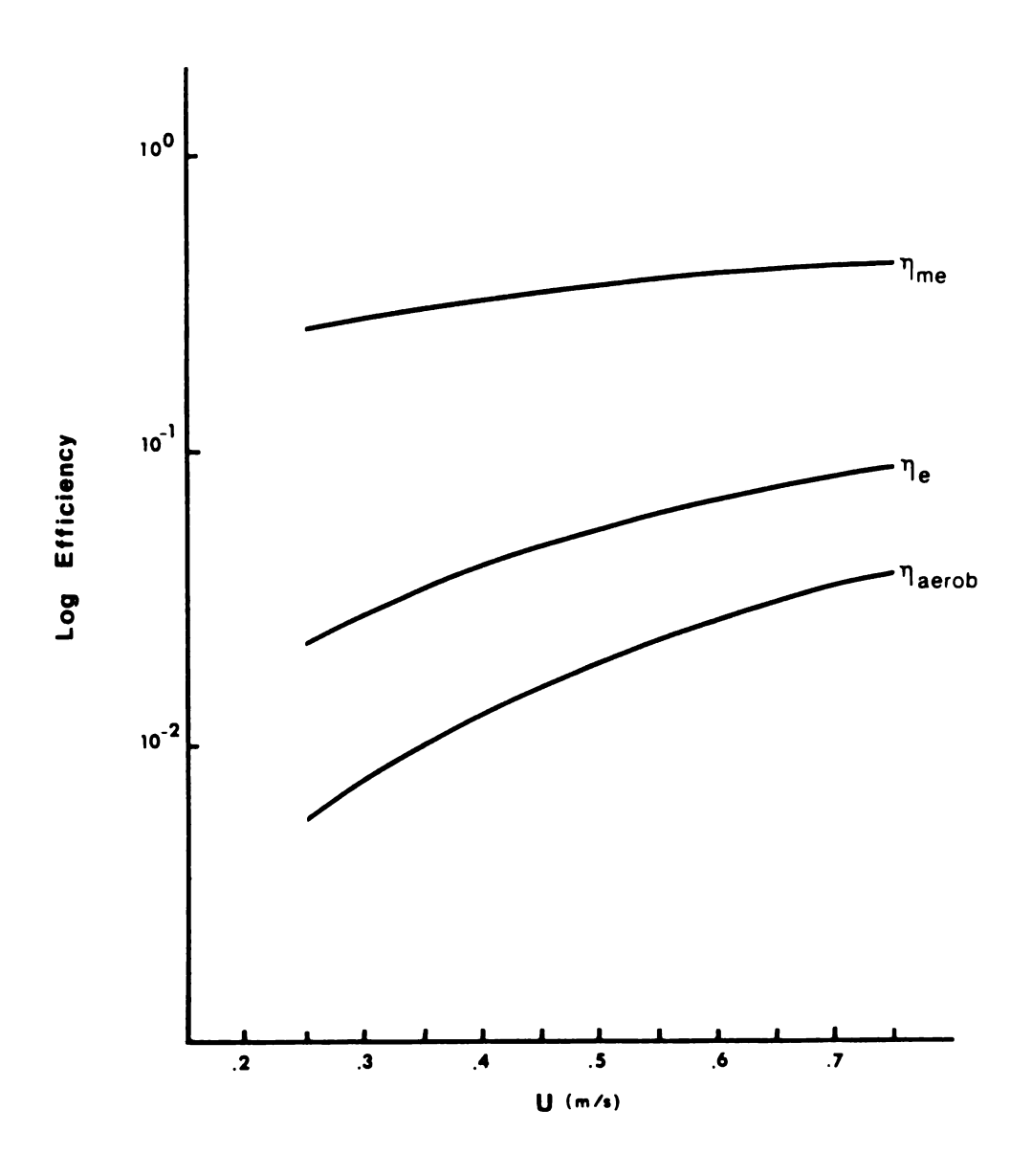
The relationship between  $E_{\mbox{tot}}$  and U (Fig. 19) is:

$$E_{tot} = 0.62U^{1.83}$$
 (43)

which was significant at P < 0.001 with a correlation coefficient of 0.87 and n = 25.

As illustrated in Fig. 19, the  $\eta_e$  was found to increase steadily with increasing U. With regard to  $\eta_{aerob}, \eta_e$  was 2.5 to 3.9 times larger. This difference is due to the

Figure 19. The logs of efficiencies ( $\eta_{me},\,\eta_{e},$   $\eta_{aerob})$  as a function of swimming velocity, U.



additional energy needed during the stroke for the recovery phase and acceleration and deceleration of the hindfeet which is taken into account in the computation of  $\eta_e$ .

Webb (1975b) calculated the  $\eta_{\rm aerob}$  for rainbow trout and sockeye salmon at 0.15 and 0.22, respectively. At slow speeds the efficiency for trout was low, which Webb (1971a) suggested as the reason for the fish's reluctance to swim at these low velocities.

Contrary to organisms that propel themselves by lateral undulations, paddle-propulsive organisms, such as the muskrat, are not as efficient in the conversion of metabolic energy to propulsive power. For surface swimmers such as the duck (Prange and Schmidt-Nielsen, 1970) and humans (DiPrampero et al., 1974) maximum values of  $\eta_{aerob}$  were 0.047 and 0.052, respectively, which were higher than the muskrat. This difference is probably due to the higher metabolic scope experienced by swimming humans and ducks.

Prange (1976) found the  $\eta_{aerob}$  for green sea turtles to reach a maximum value of 0.09 at a swimming velocity of 0.35 m/s. This high value is not too surprising because the sea turtle derives thrust in both power and recovery strokes of the forelimb (Walker, 1971). Comparable efficiencies are found in other organisms which utilize a lift-based propulsive mechanism, such as the fish Cymatogaster with a aerob of 0.12 to 0.13 (Webb, 1975b). These values are believed to be lower than efficiencies of caudal fin propulsors due to the energy necessary for rotating and accelerating the pectoral appendages (Webb,

1975b). Weis-Figh (1972) calculated that 43 percent of the total mechanism power expenditure was lost to the inertia of hummingbird wings at a normal wing beat frequency while hovering.

The mechanical efficiency of paddling propulsion in the muskrat was estimated from the model presented by Blake (1979, 1980a,b). Unlike the calculations by Webb (1975b), which employ aerob and estimates the muscular efficiency, Blake's model relies on the computation of energetics throughout the stroke cycle. The mechanical efficiency,  $\eta_{\text{tile}}$ , is computed by:

$$\eta_{\text{me}} = E_{\text{th}}/E_{\text{tot}}$$
(44)

and is illustrated in Fig. 19 over the range of test velocities. With increasing U,  $\eta_{me}$  increased steadily from 0.25 to 0.44. The maximum value of  $\eta_{me}$  for the muskrat was 75 percent higher than the mechanical efficiency of fish using labriform locomotion (Blake, 1980a). Blake reported an 11 percent reduction in the efficiency from the power to recovery phase. In the case of the muskrat, the energy expended in the recovery phase was responsible for a significant reduction in  $\eta_{me}$ . Compared to the angel fish in which frictional drag predominated in the recovery phase, high pressure drag during the recovery phase of the muskrat expended relatively more energy.

In contrast to fish which swim in the carangiform mode, the muskrat is inefficient in the generation of propulsive power (Webb, 1975a). The mechanical efficiency of the rainbow trout and sockeye salmon were 0.7 and 0.9 (Webb, 1975b). Wu (1971) has

suggested that under optimal conditions the propulsive efficiency for this type of fish may be as high as 97 percent. It thus appears that the paddling mode with its recovery stroke and associated energy loss is a liability in the attainment of high propulsive efficiency.

An alternate approach to the examination of efficiency is the concept of cost of transport. The cost of transport equals the mass-specific metabolic energy used to travel at a given velocity. It is proportional to the resistance of the environment and internal resistance of the body, and inversely proportional to the efficiency of locomotion (Tucker, 1970).

The net cost of transport allows for the examination of that increment of energy utilized in traversing a distance at a constant velocity. On the other hand, the gross cost of transport examines the total energy expenditure and is thus of greater importance to the organism as a whole, and will be used in this examination. Schmidt-Nielsen (1972b) and Hill (1976) have indicated that as velocity increases the resting  $\dot{V}_0$  becomes of less significance in the gross cost of transport, but is the dominant component at low velocities. In comparison, the net cost of transport may remain constant with increasing velocity, as in the case of running mammals (Hill, 1976). However, Prange and Schmidt-Nielsen (1970)

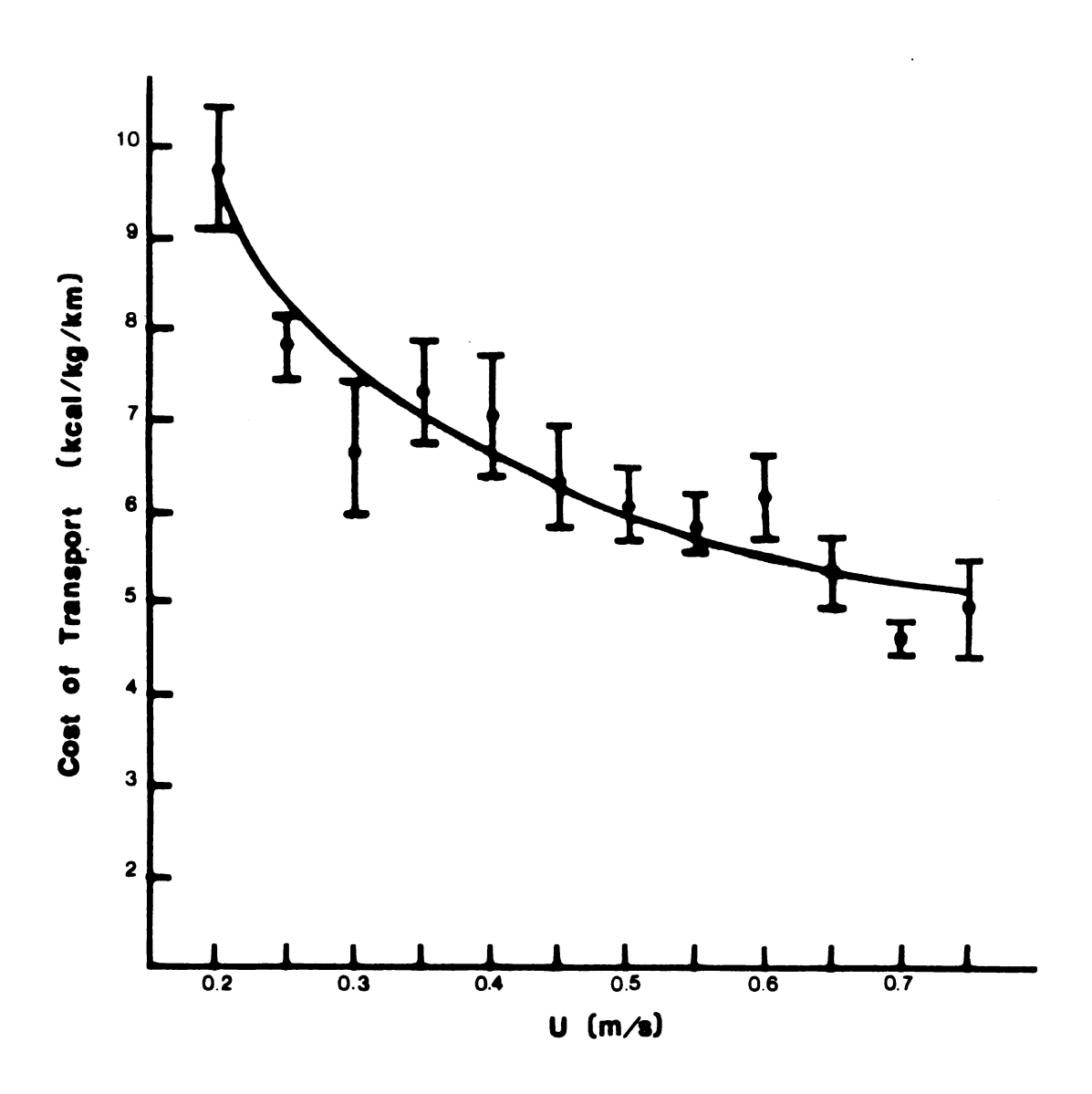
caution against the use of net cost of transport in that the assumption that the energetic requirements for maintenance are constant during elevated metabolic activity is difficult to substantiate.

Fig. 20 illustrates the relationship between the gross cost of transport and U of swimming muskrats computed from mean  $\dot{v}_{02}$  and the regression of total  $\dot{v}_{02}$  from Table 1, which were multiplied by the caloric conversion factor of 4.8 kcal/l 0<sub>2</sub>. The cost of transport showed an inverse relationship with U, with the minimum cost of transport occurring at a U of 0.75 m/s at approximately 5.1 kcal/kg/km.

It would be predicted that the muskrat would normally cruise at  $0.75 \, \mathrm{m/s}$ , where the cost of transport is minimal and  $_{\mathrm{aerob}}$  and  $_{\mathrm{me}}$  highest. This velocity would be considered to represent the optimal cruising speed,  $_{\mathrm{C}}$ , opt (Weihs, 1973; Ware, 1978), which maximizes the distance travelled for a given amount of energy expended.

Prange and Schmidt-Nielsen (1970) found that the duck normally swims at its minimum cost of transport, which occurred at a velocity of 0.48 m/s. For animals such as sea turtles (Prange, 1976) and birds (Tucker, 1971), U<sub>C</sub>, opt occurred within the range of velocities used in long migrations. In this manner, the animals were able to migrate long distances by minimizing the energetic expenditure and thus the utilization of stored fat, which ultimately limits the extent of the migration. Using cost of transport, Tucker (1975) has estimated the minimum size necessary for migration for different modes of locomotion.

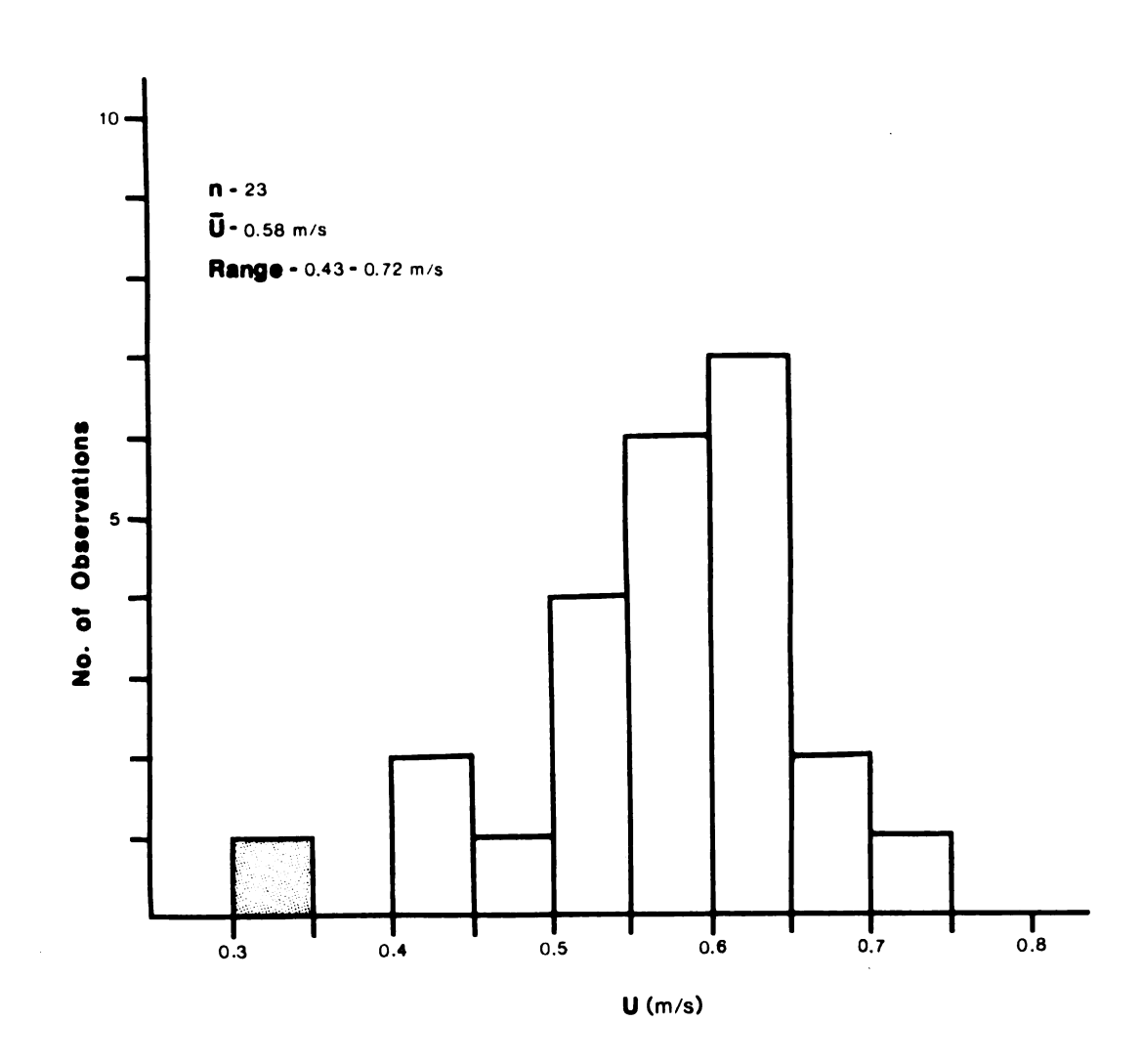
Figure 20. The gross cost of transport as plotted against swimming velocity, U. The dotted line represents the cost of transport calculated from the regression of total  $\mathring{v}_0$  from Table 1A. The solid dots represent the mean values over the range of 0.2 to 0.75 m/s. The vertical lines represent  $\pm$  one standard error (SE).



The muskrat, however, does not swim at the speed of its minimum cost of transport at 0.75 m/s, but rather was observed to cruise normally at a mean velocity of 0.58 m/s, while unrestricted in a large pond (Fig. 21). Disagreement between expected and observed swimming speeds is most likely due to the large surface drag the muskrat must overcome the mean observed velocity as indicated by a hull speed of 0.63 m/s. Above the hull speed, the increased drag necessitates an increased power input which the muskrat probably supplies through anaerobic metabolism as suggested by the fatigue in ainmals swimming at 0.7 and 0.75 m/s. Since the cost of transport approaches an asymptote with increasing U, the cost of transport is still low at 0.58 m/s compared to 0.75 m/s. Thus, by cruising at 0.58 m/s, the muskrat increases its efficiency of energy utilization, but avoids a possible oxygen debt, due to anaerobic metabolism and large drag force.

Despite the apparent advantages to swimming at 0.58 m/s, the muskrat does swim above and below this velocity. One striking example is illustrated by the stippled area on Fig. 21. In this case a muskrat was observed to swim steadily at 0.3 m/s while carrying food in its mouth. Although travelling at a slow velocity, the frequency of propulsive movements by the legs and tail increased significantly compared to animals without food. This behavior was observed at other times when the muskrat was transporting food. Because the food consisted of long filamentous pondweeds, this material probably greatly increased drag, resulting in a loss of propulsive power, which was compensated for by increased propulsive movements.

Figure 21. Numbers of observations of muskrats swimming in a large pond over a range of velocities. The single observation represented by the stippled area was for an animal observed swimming while carrying food.

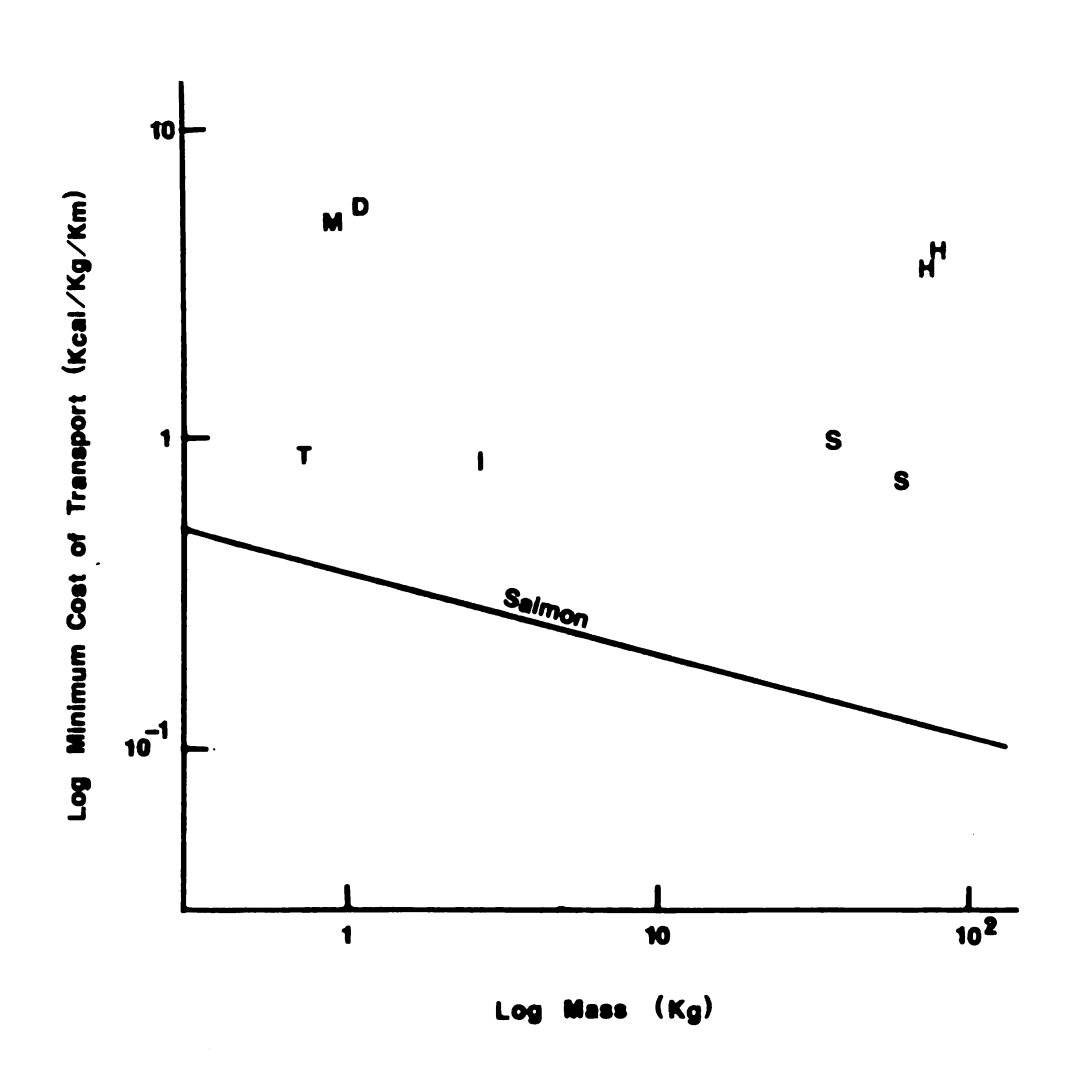


In comparison with other swimmers (Fig. 22), the minimum cost of transport for muskrats, represented by M, was exceedingly high. Although comparable to the duck (D) (Prange and Schmidt-Nielsen, 1970), the minimum cost of transport for the muskrat was 13.5 times greater than similarly sized fish as represented by the salmon (Brett, 1964). The line extrapolated for swimming salmon is the lowest minimum cost of transport found for any mode of locomotion (Schmidt-Nielsen, 1972a; Tucker, 1975). Humans (H) were relatively more inefficient than muskrats in that their minimum cost of transport was approximately 30 times that of fish (DiPrampero, pers. comm.). The remaining points illustrate values for the green sea turtle (T) (Prange, 1976), sea lions (S) (Costello and Whittow, 1975; Kruse, 1975), and marine iguana (I) (Gleeson, 1979).

It should be noted that the high costs of transport for the muskrat, duck, and humans are possibly attributable to such common factors as their paddling mode of swimming, high drag due to surface swimming, and maintenance of exercise metabolism and thermoregulation in a highly thermally conductive medium. The importance of thermoregulation is illustrated by a reduction of the aerobic energetic expenditure and consequently the cost of transport to 4.1 kcal/kg/km for muskrats in thermoneutrality at a water temperature of 30°C. This represents a 20 percent reduction from the cost of transport at 25°C in water.

The lower cost for the sea lions may be explained by a reduction in drag due to a more streamlined shape and submerged swimming (Costello and Whittow, 1975; Kruse, 1975) and use a hydrofoil type propulsor (English, 1976).

Figure 22. Comparison of the minimum cost of transport over a range of body masses. Discussion and symbols are given in the text.



Although the marine iguana (Gleeson, 1979) and sea turtle (Walker, 1971) swim using lateral undulations and subaqueous flight, respectively, which generate thrust during both power and recovery strokes, their costs of transport were still greater than fish. Because both reptiles were surface swimming, the drag due to wave formation may have imposed high energy requirements as in the mammalian paddlers. Additionally, Prange (1976) feels that for the sea turtle interruption of swimming for respiration, by using the flippers to lift the head, would reduce the overall efficiency.

The significance of surface drag becomes apparent when examining the minimum cost of transport for <u>Cymatogaster aggregata</u> which uses the labriform mode of swimming in which power and recovery strokes occur (Webb, 1973b). The minimum cost of transport computed for <u>Cymatogaster</u> from metabolic data by Webb (1975b) was found to fall on the line for salmon (Fig. 22). Thus, despite lowered mechanical efficiency of the labriform mode, the efficiency in terms of cost of transport is equivalent to that of a fish locomoting by lateral undulations. Since the body is submerged and held straight, the swimming drag could be near the theoretical minimum (Webb, 1975b), so that the loss of power due to this swimming mode does not significantly affect performance.

## Aquatic Locomotory Adaptations

In terms of morphology, the muskrat has changed little from a terrestrial form. The most significant morphological change in terms of propulsion has been the development of the hindfeet and laterally compressed tail. This section will investigate the

benefit of these structures to aquatic locomotion by the muskrat.

During paddling locomotion, the paddle must be shaped so as to maximize its drag as it is swept posteriorly in order to maximize thrust and efficiency. The optimum paddle shape is similar to a flat plate oriented normal to the direction of movement so that the water striking the paddle surface produces drag (Robinson, 1974). Counsilman (1968) has indicated that the pressure drag generated from turbulence along the downstream surface of the paddle is more important than the frontal pressure drag. Turbulence around the periphery is enhanced, by a paddle of a rectangular, oval, or fan shape (Robinson, 1975). Blake (1980b) considered that the thrust force produced by a rowing appendage during the power phase was directly proportional to a shape factor which has not been well defined. It was expected that paddling appendages would have high shape factors which aid in more effective propulsion.

In mammals the surface areas of the hindfeet which are used as paddles is increased by interdigital webbing (e.g. otter, beaver) or fringe hairs (e.g., muskrat), in conjunction with a general lengthening of the foot. Howell (1930) stated that the percentage of hindfoot length to body length for terrestrial rodents is usually less than 20 percent, while a value of 38.5 percent was reported for the muskrat. Alexander (1968) has argued that generation of thrust is most economical when the mass of water being worked on is large. The effective increase in surface area by modifications of the muskrat foot would therefore accelerate a large mass of water posteriorly, providing momentum to the animal.

In addition to the muskrat, fringed hindfeet are found in many

other small mammals such as Desmana, Galemys, Neosorex, Atophyrax, Neomys, Chimarrogale, Crossogale, Nectogale, Ichthyomys, Rheomys, and Anotomys (Howell, 1930). Howell believed that fringe hairs were not as efficient as webbing, but were undoubtedly adequate to propel a small body. In comparison to webbing, fringe hairs would not serve as an effective barrier in preventing water from passing between the digits, thereby reducing the effective surface area of the foot. However, Counsilman (1968) reported that a human hand with the fingers spread slightly produced more drag than a closed hand. Such results may be induced by an increase in turbulence between the digits increasing pressure drag (Counsilman, 1968). The muskrat may therefore utilize the fringe hairs to generate turbulence for more effective propulsion. The significance of the fringe hairs was illustrated in the present investigation by a large decrease of the drag on isolated hindfeet in which the hairs were removed.

In contrast to the power phase, in which the drag on the hindfoot should be maximized, the recovery phase should reduce the drag on the foot as much as possible. In this manner, the thrust generated during the power phase will not be cancelled during the recovery phase.

Observations of the recovery phase of the muskrat showed an adduction and plantarflexion of the digits, and supination of the entire foot. These actions tended to minimize the frontal surface area of the foot, thus reducing drag. However, the dimensions of the frontal surface are such that pressure drag probably represents the major drag component on the foot. This is also suggested by

large turbulence in the wake of the foot. In contrast, the dominant drag component is frictional during the recovery phase in angelfish (Blake, 1979, 1980a) and water beetles (Nachtigall, 1960), or there is no significant drag as in human swimmers during the Australian crawl.

Evolutionary modification of the hindfoot from a terrestrial ancestor to a semi-aquatic form could be easily accomplished. Pre-existing skin folds between the digits or the hairs on each toe could have changed to form webbed and fringed feet, respectively, by a temporal genetic mechanism (Gould, 1977). Such an elementary modification of the foot would increase the efficiency during paddling without sacrificing the organism's terrestrial performance.

Although the muskrat has evolved a foot morphology which allows it to locomote in an aquatic environment while maintaining terrestrial capabilities, it has been necessary to change its gait parameters from a terrestrial type to one which is more effective for swimming. Contrary to for terrestrial vertebrates in which  $\mathbf{t_r}$  is shorter that  $\mathbf{t_p}$  (Goslow et al., 1973; Edwards, 1980), the muskrat has a relatively long recovery phase. The recovery phase for terrestrial locomotion is "wasted" time, and a shorter  $\mathbf{t_r}$  would maximize the time that the limb contacts the substrate for more efficient propulsion (Edwards, 1980). Because the muskrat foot during the recovery phase has a large pressure component and a relative velocity that is large, due to the additive effect of and U, a long  $\mathbf{t_r}$  would reduce  $\mathbf{v'}$  to decrease  $\mathbf{dT_r}$ . The  $\mathbf{dT_r}$  would also be minimized by a decrease in the radius of the foot

through a shift of  $C_{\mathbf{A}}$  due to plantarflexion of the digits and retraction of the femur to bring the rotation point closer to  $C_{\mathbf{A}}$ .

Increased thrust for the muskrat at higher values of U is dependent on the arc through which the foot passes during the power phase. Unlike certain lateral undulatory propulsors, where the amplitude of the propulsive unit is held constant and the frequency varied (Hunter and Zweifel, 1961), and unlike other semi-aquatic mammals (Mordvinov, 1977), muskrats in the present study maintained a constant frequency.

A constant stroke frequency suggests the possibility of a resonating system operating in aquatic locomotion of the muskrat. Such systems have been hypothesized in terrestrial locomotion (Taylor, 1978). Such resonant systems are believed to reduce the energetic expenditure for locomotion by storage of elastic energy in the muscles and tendons (Dawson and Taylor, 1973; Taylor, 1978).

Stored elastic energy could potentially be utilized to reaccelerate the muskrat limb in the transition period between recovery and power phases. An increase in arc with increasing U would tend to stretch the muscle fibers and tendons allowing for greater elastic storage.

Heglund et al. (1974) found that the galloping frequency of terrestrial mammals varied in direct response to body weight, such that:

frequency = 
$$269M_b^{-0.14}$$
 (45)

where the frequency is in strides/min and M<sub>b</sub> in kg. For the muskrat, the measured frequency was found to be 91 percent lower than the frequency predicted by equation (45). The discrepancy may be due to the use of the trunk musculature in the transition from trot to gallop in terrestrial locomotion (Taylor, 1978), while the swimming muskrat uses only its limb muscles for propulsion. Additionally, equation (45) was determined for terrestrial mammals, while the muskrat locomotes in an aquatic environment.

Howell (1930) reviewed the morphology and function of the tail in various aquatic mammals. A number of semi-aquatic representatives of the orders Insectovora and Rodentia possess a laterally compressed tail. The depth of the tail is often increased by either a fleshy keel (e.g., Ondatra, Potomogale, Desmana) or a keel of stiff hairs (e.g., Neomys, Nectogale).

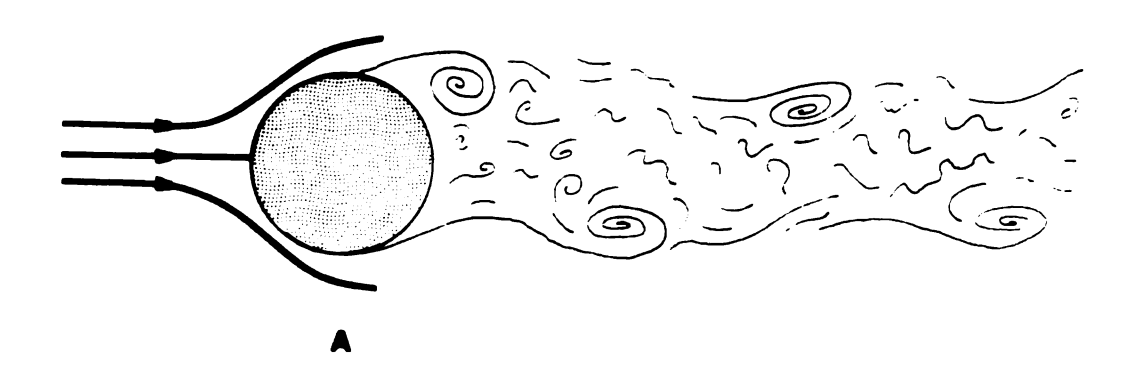
The function of the tail in aquatic locomotion has been under considerable debate, especially in the case of the muskrat.

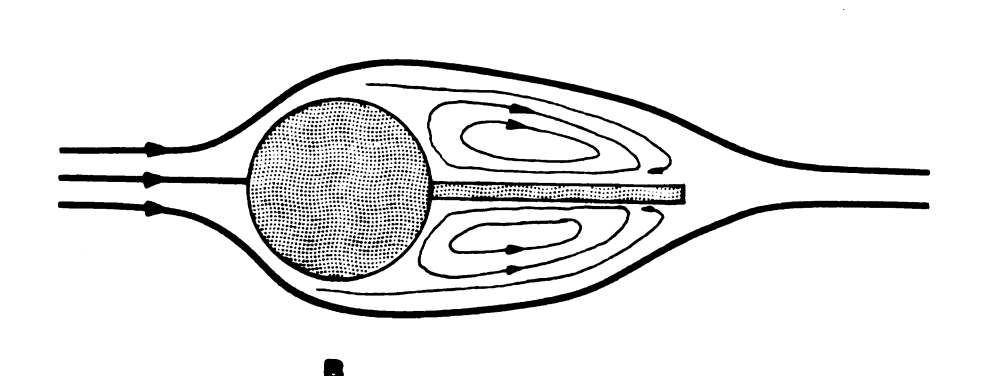
Because no rigorous study has been made on swimming in muskrats, the majority of observations on muskrats and the tail have been reported in an almost anecdotal manner.

Various authors (Howell, 1930; Kirkwood, 1931; Svihla and Svihla, 1931; Mizelle, 1935) have reported that during surface swimming the tail was held straight with no apparent propulsive function. A laterally compressed tail in this position may act as a drag reduction device by functioning as a "splitter" plate by decreasing turbulence in the wake.

The effect of a splitter plate is illustrated in Fig. 23. For a bluff (or non-streamlined) body in a laminar flow regime in which

Figure 23. Illustration of the flow around a circular body with (A) and without (B) a splitter plate.





inertial forces dominate (Fig. 23A), a pressure differential is established along the surface of the body due to a change in the momentum of the water. This results in a separation of the flow from a point on the contour of the body so that the main flow is divided from the recirculating flow posterior to the body (Potter and Foss, 1975). Separation of flow is responsible for such phenomena as "stall" on an aircraft and large drag on bluff bodies.

Because the separation point is not stationary but oscillates around an average location, a vortex is generated as the separation point moves (Potter and Foss, 1975). The vortices formed on each side of the body moving downstream have opposite directions of rotation and are symmetrically staggered (Prandtl and Tietjens, 1934). The energy necessary to maintain this vortex arrangement (Karmen vortex street) is manifested as an increase in the drag on the body.

Fig. 23B illustrates the flow pattern around a bluff body with a splitter plate. In this instance, the splitter plate is oriented vertically behind the body. The action of this device is to align equally the vortices posterior to the body (Hoerner, 1965). This is accomplished by the plate's resisting interference between the stagnant recirculating water masses, so that they act as solid tapering extensions of the body. The effect is to permit a smooth transition of water momentum over the body and prevent turbulence and energy loss in the wake. Therefore, splitter plates tend to streamline the body effectively.

Although it was originally hypothesized in this study that the

outstretched tail of the muskrat would function as a splitter plate for drag reduction, this was not borne out by flow visualization experiments. Ink injected into the water flow about a frozen muskrat showed recirculation and vortex formation directly downstream of the body. However, cross-over flow around the tail and a vortex street in the wake signified that the tail was not of a great enough dorso-ventral height to perform as a splitter plate. Vortex streets were also observed for muskrats swimming unrestricted in a large pond through a mat of duckweed (Lemna sp.). However, in this case the tail was observed to move laterally, which may have been responsible for generation of the vortex pattern.

The motion of the laterally compressed tail as observed in the water channel and artificial ponds was similar to anguilliform swimming in fish. The anguilliform mode is characterized by the generation of travelling waves with more than one-half wavelength within the body (Breder, 1926). The wave is produced through serial contraction of myomeres in fish (Grillner, 1974). For the muskrat, long tendons insert along the length of the tail and assist in lateral flexion. To produce the travelling wave pattern observed in swimming, the tail probably acts as a hybrid oscillator as proposed by Blight (1977) where the tail is stiff at the base and flexible toward the tip. Thus it is the resistance of the water against the sides of the tail as it is muscularly flexed that provide the wave sequence.

The thrust power generated by lateral undulations of the tail was maximum at only 1.4 percent of the power needed to propel the

muskrat at 0.75 m/s (Table 2). The proportion of thrust generated by the tail appears far too small to be significant in the overall energy budget. This then leaves the question of what were the selective pressures responsible for the development of a laterally compressed tail in several species of semi-aquatic mammals.

For a well insulated endothermic homeotherm such a the muskrat a compressed tail could give a high surface-to-volume ratio. The tail is then capable of acting as an effective thermoregulatory device for the control of whole-body insulation (Fish, 1979). However, terrestrial mammals do not possess unfurred, compressed tails for thermoregulation, and several species of semi-aquatic mammals have tails which assume a compressed shape by the addition of fringe hairs rather than a fleshy keel. It therefore seem unlikely that laterally compressed tails in semi-aquatic mammals have evolved solely in response to thermoregulatory needs, and that a hydrodynamic explanation may be more appropriate.

Webb (1973a) has suggested that the deep caudal fin found in most fish has evolved for high acceleration and high speed maneuverability. Since muskrats in the present study were only allowed to swim in a straight path, it was impossible to judge whether they used their tails for maneuverability. However, this may still be a viable possibility.

Fast-start performance as a means of evaluating acceleration was examined by applying an electric shock stimulus to a single resting muskrat over ten trials. The response of the muskrat was filmed at 50 frames/s. When it was shocked, the muskrat vertically flexed its tail and body so that the posterior part of the body was

oriented at approximately 90° to the horizontal. Upon extension of the body, the hindfeet were used in unison with a slight lag by one of the feet. This action rapidly accelerated the muskrat forward. At this time the tail, although showing a large lateral displacement, was flexed until the body was totally extended and the paddling cycle had resumed in the hindfeet.

In this instance, a laterally compressed tail did not appear to function in generating increased thrust during rapid starts. However, a dorso-ventrally flattened tail could effectively generate thrust for acceleration through rapid flexion and extension of the body. For mammals such as otters, sirenians, and cetaceans, which possess a depressed tail and move by flexion and extension of the body (Parry, 1949; Tarasoff et al., 1972; Hartmann, 1979), the suggestion by Webb (1973a) for the evolution of expanded tails may have validity.

The use of a compressed tail for acceleration may be valid in that acceleration by muskrats swimming against a constant water current was often accompanied by an increase in paddling frequency and amplitude of the tail. With such an increase in the wave parameters of the tail it would be expected that thrust would increase. Such a situation would also exist when muskrats swim while carrying food.

One muskrat which had its tail surgically removed appeared to accelerate more slowly than intact animals. The most significant observation on this animal occurred at the higher velocities. Without its tail, slight yawing motions were seen. These yawing motions were probably the direct result of the alternating strokes

of the feet in the paddling mode. Due to the imbalance of forces form the recovery and power phases, a torque develops about the center of the pelvic region resulting in rotation of the head toward the power phase side. In animals with intact tails which are synchronous with the hindfoot stroke, the base of the tail moves to the side opposite the hindfoot which is initiating the power phase so that lateral forces from the tail could counterbalance the yawing.

Yawing would also be kept to a minimum due to the morphology of the muskrat. With the vertical orientation of the hindfeet for paddling and high drag on the recovery phase foot due to its relative velocity and dimensions, the torque would be reduced, but still at a large cost to the net thrust. In addition, the paddle propulsor is situated at the posterior end of the body providing a large inertial mass to oppose yaw, similar to deep bodied fish (Lighthill, 1969).

Thus it appears that the laterally compressed tail in muskrats functions to assist in the effective generation of thrust. This is accomplished through lateral undulations which generate a small thrust in conjunction with reduced drag by preventing yaw and possible flow modifications.

## **CONCLUSIONS**

In comparison to highly adapted aquatic organisms, the muskrat may be regarded as an inefficient swimmer in both physiological and morphological parameters. This appears to be largely due to its paddling mode of surface swimming.

Morphologically, the apparent aquatic adaptations such as the fringe of stiff hairs on the hindfeet and laterally compressed tail appear by themselves to be ineffective in the generation of thrust in the muskrat compared to structures found in more aquatically adapted vertebrates. Mayr (1956) has argued for multiple solutions for biological needs in the evolution of organisms and noted that slight changes may be of adaptive significance. Thus, small amounts of thrust generated and/or drag reduced by the compressed tail may work in conjunction with the fringed paddling feet to increase the propulsive efficiency of the muskrat giving it a selective advantage over terrestrial forms in an aquatic habitat. This is consistent with the holistic views of Dullemeijer (1974) in which the organism represents the total of functional units which act together as subsets within the organism.

In comparison to swimming by lateral undulations and lift-based mechanisms, the paddling mode is mechanically inefficient. This is due to the substantial energy loss in the recovery phase of the stroke cycle, and acceleration of the feet at

the ends of the cycle. Conformational and temporal changes in the hindfoot during the recovery phase reduce the energy loss and decrease the negative thrust against the power phase which is responsible for the generation of thrust.

The thrust force generated during the power phase is maximized by increasing the plantar surface area of the hindfeet through a general lengthening of the digits and lateral fringe hairs and increased arc through which the feet are swept.

The paddling mode itself, while relatively inefficient, permits the muskrat to effectively generate propulsive forces while swimming at the surface. The evolution of this mode represents only a slight modification from a terrestrial type of locomotion, which thus takes account of the heritage of the species (Mayr, 1956). Additionally, the presence of non-wettable fur on small semi-aquatic mammals, although providing insulation, gives the animals a large buoyant effect, thus decreasing the energy expended to float at the surface. However, the buoyancy due to the air entrapped in the dense pelage would require a large energy expenditure in order for the animal to submerge itself to a level where it could utilize a more efficient mode of swimming than paddling. Large mammals which swim submerged utilizing more efficient swimming modes possess a blubber layer to supply buoyancy. A blubber layer would be effective for large mammals, whereas buoyancy control by non-wettable fur would be limited by surface allometry and depth due to the effects of pressure on the entrapped air.

The energetic demands of paddling locomotion are large with

respect to swimming modes which maintain a mearly continuous thrust force over the entire propulsive cycle. Additionally, the large energy requirement for paddling as exemplified by the muskrat would be mandated by the increased drag due to the formation of waves at the surface. However, muskrats may reduce their energetic expenditure by swimming at speeds in which the energy demand is a low for the distance traversed. Indeed, the aerobic efficiency is maximized and the cost of transport approaches a minimum at 0.58 m/s in which unrestricted muskrats were observed to freely cruise. Swimming at this velocity would allow the muskrat to efficiently utilize its power input, while avoiding increased metabolism through anaerobiosis in response to increased wave drag above 0.63 m/s where it is predicted to be maximal.

Because of the metabolic and mechanical inefficiencies of the padoling mode and substantial energy loss to the wake for surface swimming, aquatic locomotion by the muskrat is costly compared to animals such as fish which maintain a high propulsive efficiency. In that the muskrat is highly mobile on land and in water, the morphology of this mammal should be viewed as a compromise of both form and function between vastly different environments. However, the musrkat's particular morphology and physiology permit this semi-aquatic rodent to exploit habitats which are inaccessible to more terrestrial mammals.

## REFERENCES

- Alexander, R. NcN. 1968. Animal mechanics. Univ. of Washington Press, Seattle. 346 pp.
- Arthur, S. C. 1931. The fur animals of Louisiana. Louisiana

  Dept. of Conservation, Bull. 18. 444 pp.
- bainbridge, R. 1958. The speed of swimming of fish as related to size and to frequency and amplitude of tail beat. J. Exp. Biol. 35: 109-133.
- Blake, R. W. 1979. The mechanics of labriform locomotion. I.

  Labriform locomotion in the angelfish (<u>Pterophyllum eimekei</u>):

  an analysis of the power stroke. J. Exp. Biol. 82: 255-271.
- analysis of the recovery stroke and the overall fin-beat cycle propulsive efficiency in the angelfish. J. Exp. Biol.
- propulsion in aquatic vertebrates. Symp. Zool. Soc., Lond.

  (in press).
- Blight, A. R. 1977. The muscular control of vertebrate swimming movements. Biol. Rev. 52: 181-218.
- Breder, C. M. 1926. The locomotion of fishes. Zoologica (N.Y.)
  4: 159-297.

- Brett, J. H. 1964. The respiratory metabolism and swimming performance of young sockeye salmon. J. Fish. Res. Bd. Can. 21: 1183-1226.
- Chappell, M. A. 1980a. Thermal energetics of chicks of arctic-breeding shorebirds. Comp. Biochem. Physiol. 65: 311-317.
- 1980b. Insulation, radiation, and convection in small arctic mammals. J. Mamm. 61: 268-277.
- Chassin, P. S., C. R. Taylor, N. C. Heglund, an H. J. Secherman.

  1976. Locomotion in lions: energetic cost and maximum aerobic capacity. Physiol. Zool. 49: 1-10.
- Clarys, J. P. 1979. Human morphology and hydrodynamics. <u>In</u> J. Terauds and E. W. Bedingfield, (eds.) Swimming III.

  Proceedings of the Third International Symposium of
  Biomechanics in Swimming. University Park Press, Baltimore
  pp. 3-41.
- Costello, R. R. and G. C. Whittow. 1975. Oxygen cost of swimming in trained California sea lion. Comp. Biochem. Physiol. 50: 645-647.
- Costill, D. L., P. J. Cahill, and D. Eddy. 1967. Metabolic responses to submaximal exercise in three water temperatures.

  J. Appl. Physiol. 22: 628-632.
- Counsilman, J. W. 1968. The science of swimming. Prentice-Hall,
  N. J. 308 pp.
- Dagg, A. I. and D. E. Windsor. 1972. Swimming in northern terrestrial mammals. Can. J. Zool. 50: 117-130.

- Dawson, T. J. and C. R. Taylor. 1973. Energetic cost of locomotion in kangaroos. Nature 246: 313-314.
- DiPrampero, P. E., P. Cerretelli, and J. Piiper. 1970. Lactic acid formation on gastrocnemius muscle of the dog and its relation to O<sub>2</sub> debt contraction. Resp. Physiol. 8: 347-353.
- \_\_\_\_\_\_, D. R. Pendergast, D. W. Wilson, and D. W. Hennie.

  1974. Energetics of swimming in man. J. Appl. Physiol. 37:

  1-5.
- Dugmore, A. R. 1914. The romance of the beaver. J. B. Lippincott Co., Philadelphia. 225 pp.
- Dullemeijer, P. 1974. Concepts and approaches in animal morphology. Van Gorcum, Assen, The Netherlands. 264 pp.
- Eble, H. 1954/55. Funktionelle Anatomie der Extremitatsmuskulatur von Ondatra zibethica. Wissensch. Zeitsch. Martin-Luther-Universitat Halle-Wittenberg Math.-Naturwiss. Reihe 4,5: 997-1004.
- Edwards, J. L. 1980. A comparative study of terrestrial locomotion in salamanders. Evol. Monogr. (in press).
- English, A. W. 1976. Limb movements and locomotor function in the California sea lion (Zalophus californianus). J. Zool.,
  Lond. 178: 341-364.
- Errington, P. L. 1962. Muskrat populations. Iowa State
  University Press, Ames, Iowa. 665 pp.
- Fairbanks, E. S. and D. L. Kilgore, Jr. 1978. Post-dive oxygen consumption of restrained and unrestrained muskrats (Ondatra zibethicus). Comp. Biochem. Physiol. 59: 113-117.

- Fish, F. E. 1979. Thermoregulation in the muskrat (Ondatra zibethicus): the use of regional heterothermia. Comp.

  Biochem. Physiol. 64: 391-397.
- Flaim, F. H. 1956. The osteology and myology of the pelvic and pectoral girdles and appendages of the mammalian genus <u>Odatra</u> (muskrat), with comparative notes on <u>Neotoma</u> (woodrat).

  Ph.D.thesis, Stanford University. 316 pp.
- Gessamen, J. A. 1972. Bioenergetics of the snowy owl (Nyctes scandiaca). Arctic Alp. Res. 4: 223-238.
- Gleeson, T. T. 1979. Foraging and transport costs in the

  Galapagos marine iguana, Amblyrhychus cristalus. Physiol.

  Zool. 52(4): 549-557.
- Gordon, M. S., C. Loretz, P. Chow, and M. Vojkovich. 1979.

  Patterns of metabolism in marine fishes using different modes of locomotion. Amer. Zool. 19: 897.
- Goslow, G. E., Jr., R. M. Reinking, and D. G. Stuart. 1973. The cat step cycle: hind limb joint angles and muscle lengths during unrestrained locomotion. J. Morph. 141: 1-41.
- Gould, S. J. 1977. Ontogeny and phylogeny. The Belknap Press, Cambridge, Mass. 501 pp.
- Gray, J. 1933. Studies in animal locomotion. I. The movement of fish with special reference to the eel. J. Exp. Biol. 10: 88-104.
- powers of the dolphin. J. Exp. Biol. 13: 192-199.
- Grillner, S. 1974. On the generation of locomotion in the spinal dogfish. Exp. Brain Res. 20: 459-470.

- Hall, E. R. and K. R. Kelson. 1959. The mammals of North America.

  The Ronald Press Co., New York. N.Y. 1078 pp.
- Hart, J. S. 1962. Mammalian cold acclimation. <u>In Hannon, P. and E. Viereck (eds.)</u>, Comparative physiology of temperature regulation. II. Arctic Aeromed. Lab., Fort Wainwright, Alaska. pp. 203-230.
- physiology of thermoregulation. Vol. II. Academic Press,
  New York, pp. 1-149.
- Hartmann, D. S. 1979. Ecology and behavior of the manatee

  (Trichechus manatus) in Florida. Amer. Soc. Namm. Spec.

  Publ. No. 5: 1-153.
- Heglund, N. C., C. H. Taylor, and T. A. McMahon. 1974. Scaling stride frequency and gait to animal size: mice to horses.

  Science 186: 1112-1113.
- Hertel, H. 1966. Structure, form, and movement. Reinhold, New York. 251 pp.
- Hill, R. W. 1972. Determination of oxygen consumption by use of the paramagnetic oxygen analyzer. J. Appl. Physiol. 33: 261-263.
- approach. Harper and Row, New York, N.Y. 656 pp.
- Hoerner, S. F. 1965. Fluid dynamic drag. Published by author.

  Midland Park, New Jersey. 432 pp.
- Holmer, I. 1972. Oxygen uptake during swimming in man. J. Appl. Physiol. 33: 502-509.

- Howell, A. B. 1930. Aquatic Mammals. C. C. Thomas, Springfield, Ill. 338 pp.
- Hunter, J. R. and J. R. Zweifel. 1971. Swimming speed, tail beat frequency, tail beat amplitude and size in jack mackerel,

  Trachurus synnetrucys, and other fishes. Fish. Bull. 69:
  253-266.
- Johansen, K. 1962a. Buoyancy and insulation in the muskrat. J. Manm. 43: 64-68.
- 1962b. Heat exchange through the muskrat tail.

  Evidence for vasodilator nerves to the skin. Acta Physiol.

  Scand. 55: 160-169.
- Johnson, C. E. 1925. The muskrat in New York. Roosevelt Wild Life Bull. 3: 199-320.
- Kermack, K. A. 1948. The propulsive powers of blue and fin whales. J. Exp. Biol. 25: 237-240.
- Kirkwood, F. C. 1931. Swimming of the muskrat. J. Mamm. 12: 317-318.
- Kruse, D. H. 1975. Swimming metabolism of California sea lions,

  Zalophus californianus. M.S. Thesis. San Diego State

  University. 53 pp.
- Lang, T. G. 1975. Speed, power, and drag measurements of dolphins and porpoises. In T. Y. Wu, C. J. Brockaw, and C. Brennan (eds.), Swimming and flying in nature, Plenum Press, New York and London, pp. 553-572.
- and D. A. Daybell. 1963. Porpoise performance tests in a seawater tank. Nav. Ord. Test Stat. Tech. Rep. 3063: 1-50.

- Lighthill, M. J. 1969. Hydromechanics of aquatic animal propulsion. Ann. Rev. Fluid Mech. 1: 413-446.

  1970. Aquatic animal propulsion of high hydrodynamic efficiency. J. Fluid Mech. 44: 265-301.

  MacArthur, R. A., 1979. Seasonal patterns of body temperature and
- MacArthur, R. A., 1979. Seasonal patterns of body temperature and activity in free ranging muskrats (<u>Ondatra zibethicus</u>). Can.

  J. Zool. 57: 25-33.
- Mayr, E. 1956. Geographic character gradients and climatic adaptation. Evolution 10: 105-108.
- McEwan, E. H., N. Aitchison, and P. E. Whitehead. 1974. Energy metabolism of oiled muskrats. Can. J. Zool. 52: 1057-1062.
- Mizelle, J. D. 1935. Swimming of the muskrat. J. Mamm. 16: 22-25.
- Mordvinov, Y. E. 1974. The character of boundary later in the process of swimming in the muskrat (<u>Ondatra zibethica</u>), and mink (<u>Mustela lutreola</u>). Zool. Zh. 53: 430-435. (in Russian).
- effectiveness of propelling systems for some aquatic mammals.

  Zool. Zh. 55(9): 1375-1382. (in Russian).
- semiaquatic mammals on parameters of locomotor cycle of motile organs and their areas. Vestnik Zoologii 5: 54-60. (in Russian).
- Mount, L. E. and J. V. Willmont. 1967. The relation between spontaneous activity, metabolic rate and the 24 hour cycle in mice at different environmental temperatures. J. Physiol. 190: 371-380.

- Muller, G. 1952/53. Betrage zur Anatomie der Bisamratte (Ondatra zibethica). I. Einfuhrung, Skelett und Literature. Wiss.

  Z. Univ. Halle, Math-Nat. 2: 817-865. Nachtigall, W. 1960.
- Uber Kinematik, Dynamik und Energetik des
  Schwimmens einheimischer Dytisciden. Z. vergl. Physiol. 43:
  48-118.
- Nadel, E. H. 1977. Thermal and energetic exchanges during swimming. In E.R. Nadel (ed.), Problems with temperature regulation during exercise. Academic Press Inc., New York. pp. 91-119.
- , I. Holmer, U. Bergh, P. O. Astrand, and J. A. J. Stolwijk.

  1974. Energy exchanges of swimming man. J. Appl. Physiol.

  36: 465-471.
- Parry, D. A. 1949. The swimming of whales and a discussion of Gray's paradox. J. Exp. Biol. 26: 24-34.
- Pasquis, P., A. Lacaisse, and D. Dejours. 1970. Maximal oxygen uptake in four species of small mammals. Resp. Physiol. 9: 298-309.
- Peterson, A. W. 1950. Backward swimming of muskrat. J. Mamm. 31: 453.
- Peterson, R. T. 1968. The birds. Life Nature Library. Time Inc., New York. 192 pp.
- Potter, M. C. and J. F. Foss. 1975. Fluid mechanics. Ronald Press Co., New York. 586 pp.
- Prandtl, L. and O. G. Tietjens. 1934. Applied hydro and aeromechanics. (New ed. 1957), Dover Books, New York, N. Y. 311 pp.

- Prange, H. D. 1976. Energetics of swimming of a sea turtle. J. Exp. Biol. 64: 1-12.
- and K. Schmidt-Nielsen. 1970. The metabolic cost of swimming in ducks. J. Exp. Biol. 53: 763-777.
- Robinson, D. E., G. S. Campbell, and J. R. King. 1976. An evaluation of heat exchange in small birds. J. Comp. Physiol. 105: 153-166.
- Robinson, J. A. 1975. The locomotion of plesiosaurs. N. Jb. Geol. Palaont. Abh. 149: 286-332.
- Ruben, J. A. and D. E. Battalia. 1979. Aerobic and anaerobic metabolism during activity in small rodents. J. Exp. Zool. 208: 73-76.
- Schiehauf, R. E., Jr. 1979. A hydrodynamic analysis of swimming propulsion. In J. Terauds and E. W. Bedinfield (eds.),

  Swimming III. Proceedings of the Third International

  Symposium of Biomechanics in Swimming. University Park Press,

  Baltimore. pp. 70-109.
- Schmidt-Nielsen, K. 1972a. Locomotion: energy cost of swimming, flying and running. Science 177: 222-228.
- Press, London. 114 pp.
- Shcheglova, A. I. 1964. Specific features of heat exchange in the muskrat. Ref. Zh. Biol. No. 71245. (in Russian).
- Simpson, G. G., A. Roe, and R. C. Lewontin. 1960.

  Quantitative zoology. Harcourt, Brace, and World, Inc.,

  New York. 440 pp.

- Steele, R. G. D. and J. H. Torrie. 1960. Principles and procedures of statistics. McGraw-Hill, New York. 481 pp.
- Svihla, A. and R. D. Svihla. 1931. The louisiana muskrat.

  J. Namm. 12: 12-28.
- Tarasoff, F. J., A. Bisaillo, J. Pierard, and A. P. Whitt. 1972.

  Locomotory patterns and external morphology of the river

  otter, sea otter, and harp seal (Mammalia). Can. J. Zool.

  50: 915-929.
- Taylor, C. R. 1978. Why change gaits? Recruitment of muscles and muscle fibers as a functin of speed and gait. Amer. Zool. 18: 153-161.
- Taylor, G. 1952. Analysis of the swimming of long narrow animals, Proc. R. Soc. Lond., Ser. A Biol. Sci. 214: 158-183.
- Thomas, D. P., G. F. Fregin, N. H. Gerber, and N. B. Ailes. 1980.

  Cardiorespiratory adjustments to tethered-swimming in the horse. Pflugers Arch. (in press).
- Tucker, V. A. 1970. Energetic cost of locomotion in animals.

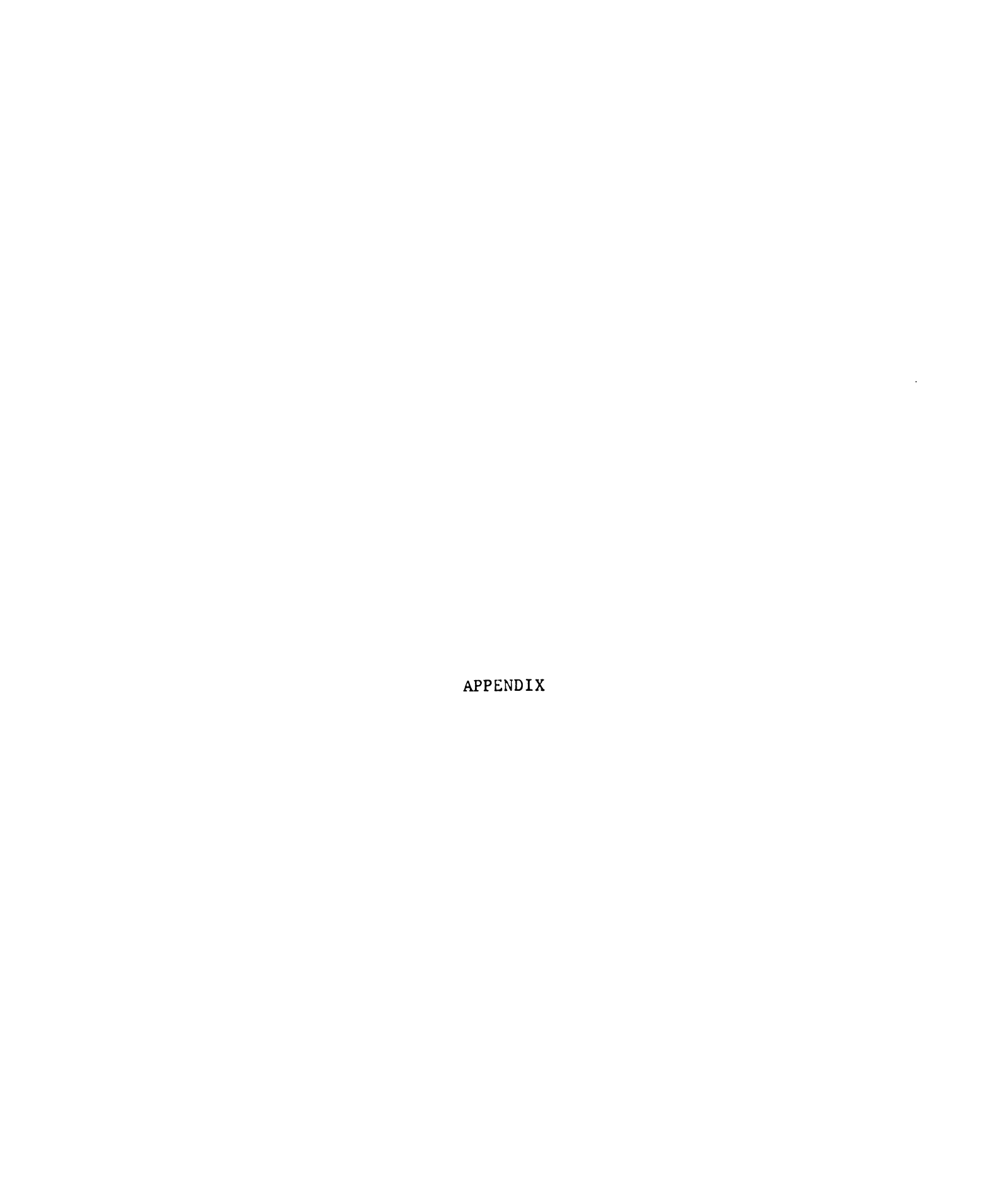
  Comp. Biochem. Physiol. 34: 841-846.
- 1971. Flight energetics in birds. Amer. Zool. 11:
- 1975. The energetic cost of moving about. Amer. Scientist 63: 413-419.
- Vogel, S. and M. LaBarbera. 1978. Simple flow tanks for research and teaching. Bioscience 28: 638-643. Walker, E. P. 1975.
- Walker, E. P. 1975. Mammals of the world. 3rd ed. John Hopkins Press, Baltimore, Maryland. Vol. II. 1500 pp.

Walker, W. F., Jr. 1971. Swimming in sea turtles of the family Cheloniidae. Copeia 1971: 229-233. Ware, D. M. 1978. Bioenergetics of pelagic fish: theoretical change in swimming speed and ration with body size. J. Fish. Res. Bd. Can. 35: 220-228. Webb, P. W. 1971a. The swimming energetics of trout. I. and power output at cruising speeds. J. Exp. Biol. 55: 489-520. 1971b. The swiming energetics of trout. II. Oxygen consumption and swimming efficiency. J. Exp. Biol. 55: 521-540. 1973a. Effects of partial caudal-fin amputation on the kinematics and metabolic rate of underyearling sockeye salmon (Oncorhynchus nerka) at steady swimming speeds. J. Exp. Biol 59: 565-581. 1973b. Kinematics of pectoral fin propulsion in Cymatogaster aggregata. In T. Y. Wu, C. J. Brokaw, and C. Brennen (eds.), Swimming and Flying in nature. Vol. 2. Plenum Press, New York. pp. 573-584. 1975a. Hydrodynamics and energetics of fish propulsion. Bull. Fish. Res. Bd. Can. 190: 1-159. 1975b. Efficiency of pectoral-fin propulsion of Cymatogaster aggregata. In Wu, T. Y., C. J. Brokaw, and C. Brennen (eds.), Swimming and flying in nature. Vol. 2. Plenum Press, New York. pp. 573-584. 1978. Hydrodynamics: nonscombroid fish. In W. S. Hoar, and D. J. Randall (eds.). Fish physiology, Vol. VII.

Academic Press, New York. pp. 190-237.

- Weihs, D. 1973. Optimal cruising speed for migrating fish.

  Nature 245: 48-50.
- Weis-Fogh, T. 1972. Energetics of hovering flight in hummingbirds and Drosophila. J. Exp. Biol. 56: 79-104.
- Wu, T. Y. 1971. Swimming of a waving plate. J. Fluid Mech. 10: 321-344.
- Wunder, B. A. 1970. Energetics of running activity in Merriam's chipmunk, <u>Eutamias merriami</u>. Comp. Biochem. Physiol. 33: 821-836.



## APPENDIX A

List of symbols used in this study with units given in parentheses.

```
- power phase paddle plantar surface (m<sup>2</sup>)
Α
       - recovery phase paddle frontal surface (m<sup>2</sup>)
A 1
       - acceleration (m/sec<sup>2</sup>)
       - drag balance mounting bracket
В
C_{\Delta}
     - center of action for power phase
    - center of action for recovery phase
C<sub>A</sub>'
     - normal force coefficient for power phase
C_n
Cn' - normal force coefficient for recovery phase
       - maximum chord of hindfoot (m)
       - drag (N)
d
       - power stroke oar drag (N)
d'
       - recovery stroke oar drag (N)
    - maximum tail depth (m)
dт
    - energy expended during power phase to accelerate m_a (J)
E_a' - energy expended during recovery phase to accelerate m_a
         (J)
E_{D}
    - body drag energy (J)
    - energy expended during power phase to accelerate m_f (J)
Ef
Ef' - energy expended during recovery phase to accelerate mf
         (J)
E_M - metabolic energy (J)
Eρ
    - total energy expended during power phase (J)
     - total energy expended during recovery phase (J)
Er
```

```
Ert
             - thrust energy expended during recovery phase (J)
               - thrust energy expended during power phase (J)
Eτ
E_{Th}
             - net energy necessary to generate thrust (J)
          - total energy expended over cycle (J)
Etot
dF_n
               - power hase normal force (N)
dFn'
               - recovery phase normal force (N)
F_{D}
               - power phase hindfoot normal force (N)
F_{D}
               - power phase hindfoot normal force without fringe
                   hairs (N)
               - recovery phase hindfoot normal force (N)
F_{R}
                 - gravitational acceleration (9.8 \text{ m/s}^2)
g
                 - constant (2.5)
k
               - constant (1.0)
kΤ
                 - wavelength (m)
L
                 - length of hindfoot (m)
1
1_{i}
               - in-lever (m)
               - out-lever (m)
1_{o}
               - body mass (g)
M_{\mathbf{b}}
                - virtual mass of tail (kg/m)
               - added mass of hindfoot (kg)
m_a
               - wass of hindfoot (kg)
mf
                 - samples size
n
               - drag power output (w)
P_{o}
               - tail thrust power (w)
P_{T}
                 - effective power phase paddle radius (m)
r
r'
                 - effective recovery phase paddle radius (m)
               - water temperature (°C)
T_a
```

```
- power phase thrust component (N)
dT_{D}
dT_r
               - recovery phase negative thrust component (N)
               - total cycle time (s)
t_0
               - power phase time (s)
t<sub>D</sub>
                - recovery phase time (s)
tr
U
                  - swimming or water velocity (u/s)
^{\text{U}}c, opt
                  - optimal cruising speed
                  - hindfoot velocity or oar velocity (m/s)
u
                  - backward velocity of propulsive wave in tail
V
                    (n/s)
               - mass-specific oxygen consumption (cc0_2/g/hr)
                  - resultant relative velocity (m/s)
               - power phase normal paddle velocity component
v<sub>n</sub>
v<sub>n</sub>'
               - recovery phase normal paddle velocity component
               - power phase spanwise paddle velocity component
v<sub>s</sub>
vs'
                - recovery phase spanwise paddle velocity component
W
                  - tail trailing edge lateral velocity (m/s)
                - power required to accelerate and decelerate ma
W_{\mathbf{a}}
                    (W)
Wb
               - drag balance weight (kg)
                - instantaneous rate of working during power phase
dWp
                    (J)
\overline{W}_{D}
               - mean power generated during power phase (W)
               - instantaneous rate of working during recovery
dW_r
                    phase (J)
\overline{W}_r
               - mean power generated during recovery phase (W)
             - instantaneous rate of working used for thrust
dWrt
```

during recovery phase (J)

$\overline{\mathtt{W}}_{\mathtt{rt}}$	- mean power generated for thrust during recovery
"rt	
	phase (W)
dWt	- instantaneous rate of working used for thrust
	during power phase (J)
$\overline{\mathbf{w}}_{\mathbf{t}}$	- mean power generated for thrust during power
	phase (W)
w	- relative velocity of tail (m/s)
~a	- hydrodynamic angle of attack (deg)
y	- power phase orientation angle (deg)
<i>&gt;</i> '	- recovery phase orientation angle (deg)
Naerob	- aerobic efficiency
$\eta_{e}$	- overall energetic efficiency
$ u^{\text{me}} $	- mechanical efficiency
e	- density of water (1000 kg/m $^3$ )
$\boldsymbol{v}$	- recovery phase angular velocity of hindfoot
	(rad/s)
w	<ul> <li>power phase angular velocity of hindfoot (rad/s)</li> </ul>